

# Probabilistic Feature Selection in Joint Quantile Time Series Analysis

Ning Ning<sup>a,\*</sup>

<sup>a</sup>*Department of Statistics, University of Michigan, Ann Arbor, USA.*

---

## Abstract

Quantile feature selection over correlated multivariate time series data has always been a methodological challenge and is an open problem. In this paper, we propose a general probabilistic methodology for feature selection in joint quantile time series analysis, under the name of quantile feature selection time series (QFSTS) model. The QFSTS model is a general structural time series model, where each component yields an additive contribution to the time series modeling with direct interpretations. Its flexibility is compound in the sense that users can add/deduct components for each time series and each time series can have its own specific valued components of different sizes. Feature selection is conducted in the quantile regression component, where each time series has its own pool of contemporaneous external predictors allowing “nowcasting”. Creative probabilistic methodology in extending feature selection to the quantile time series research area is developed by means of multivariate asymmetric Laplace distribution, “spike-and-slab” prior setup, the Metropolis-Hastings algorithm, and the Bayesian model averaging technique, all implemented consistently in the Bayesian paradigm. Different from most machine learning algorithms, the QFSTS model requires small datasets to train, converges fast, and is executable on ordinary personal computers. Extensive examinations on simulated data and empirical data confirmed that the QFSTS model has superior performance in feature selection, parameter estimation, and forecast.

---

\*Corresponding author  
*Email address:* patning@umich.edu (Ning Ning)

*Keywords:* Quantile Feature Selection, Multivariate Time Series Analysis,  
Bayesian Inference  
*2010 MSC:* 62H86, 62M10, 62F15

---

## 1. Introduction

We firstly give the background and motivation in Section 1.1 and then state our contributions in Section 1.2, followed with the organization of the paper in Section 1.3.

### 5 1.1. Background and motivation

In the era of “big data”, electronic devices are now involved in many social activities, and can capture, store, manipulate, and analyze vast caches of such data. Conventional statistical and econometric techniques become increasingly inadequate to deal with “Big Data” problems (Varian (2014)), such as the curse  
10 of dimensionality, large storage requirement, and high computational cost. Feature selection, also known as variable selection, attribute selection or variable subset selection, is a machine learning technique for dimensionality reduction. It aims to choose a small subset of the relevant features (variables, predictors) for use in model construction, from the original ones by removing irrelevant,  
15 redundant, or noisy features. It usually leads to better learning performance in terms of higher learning accuracy, lower computational cost, and better model interpretability. It has also been proven to be an effective and efficient way in shortening training times, improving data’s compatibility with a learning  
20 e.g. Kratsios and Hyndman (2021); Hauberg et al. (2013)).

Time series forecasting as one of the most applied data science techniques in business, have been used extensively in finance, in supply chain management, in production and inventory planning, etc. However, as the time component adds additional information, time series problems are more difficult to handle compared to other prediction tasks (Chernozhukov et al. (2018)). Feature selection  
25

in time series applications was firstly introduced and further explored in Scott and Varian (2014, 2015) in the name of the Bayesian Structural Time Series (BSTS) model, which can be used for feature selection, time series forecasting, nowcasting, inferring causal relationships, etc. Qiu et al. (2018) proposed the  
30 multivariate Bayesian structural time series (MBSTS) model, which extended the BSTS model to multivariate target time series with various components. The BSTS/MBSTS model has wide applications in health care (see, e.g., Kurz et al. (2019)), spatial analysis (see, e.g., Qiu et al. (2019)), artificial intelligence (see, e.g., Jammalamadaka et al. (2019)), cryptocurrency (see, e.g., Jalan et al.  
35 (2019)), medicine (see, e.g., Talaei-Khoei et al. (2019)), environmental science (see, e.g., Droste et al. (2018)), renewable energy (see, e.g., Jiang et al. (2013)), political analysis (see, e.g., Xu (2017)), time series analysis (see, e.g., Qiu et al. (2020)), social media (see, e.g., Welbers and Opgenhaffen (2018)), marketing (see, e.g., Brodersen et al. (2015)), etc.

40 One can think of the future value of a univariate time series as a random variable whose distribution is the forecast distribution. Analogously, the future values of multivariate time series can be thought of as correlated random variables with the joint forecast distribution. The usual time series forecast is often to predict the mean or the median of the (joint) forecast distribution,  
45 which can be categorized as a point forecast. The (joint) quantile forecast is an interval forecast appealing in many economic applications (Chernozhukov and Hansen (2005)), such as value at risk in the finance industry in order to develop a strategy for trading and/or hedging purposes (more explanations can be seen in Section 6). It is to generate a range of specified coverage probability under  
50 the (joint) forecast distribution. That is, the 95% prediction interval is defined by the 2.5% and 97.5% quantiles of the (joint) forecast distribution, and the 80% prediction interval is defined by the 10% and 90% quantiles of the (joint) forecast distribution. It is an open question so far on how to incorporate the feature selection technique in joint quantile time series analysis, which is our  
55 goal of this paper.

## 1.2. Our contributions

In this paper, we propose a general probabilistic methodology for feature selection in joint quantile analysis with multivariate correlated time series data, under the name of quantile feature selection time series (QFSTS) model. Our  
60 contributions are four-fold:

- **General model structure.** First, the QFSTS model is a structural time series model, which further belongs to state space models. All state components are assembled independently, and each component yields an additive contribution to the time series modeling with direct interpretations.  
65 The flexibility of the model allows users to include different model components for each target series, such as one time series has a trend component and a regression component and another correlated time series only has a regression component. Given that our main goal is to illustrate the feature selection methodology in joint quantile time series analysis, we  
70 only illustrate using a trend time series component, a regression component and an error term (equation (1)) for simplicity, while users can add on additional time series components directly as that in Qiu et al. (2018).  
Second, the QFSTS model allows “nowcasting” and each time series can have its own pool of contemporaneous external predictors. For reasons of  
75 cost, effort, or convention, many economic time series are reported infrequently such as on a monthly or quarterly basis, despite being theoretically observable on finer time scales Scott and Varian (2014). Time series are also frequently revised after they are first reported, as new information becomes available. “Nowcasting” is to forecast a current value instead  
80 of a future value (Banbura et al. (2011)). An effective nowcasting model considers both the past behavior of the series being modeled and the values of more easily observed contemporaneous signals. All predictors in the regression component of the QFSTS model can be contemporaneous with a known lag by shifting the corresponding predictors in time. The  
85 QFSTS model allows each time series to have its own pool of predictors,

for example one time series has 50 predictors and another time series has 20 predictors of different values. Feature selection is conducted among each times series' pool of predictors while still considering the correlations among different times series.

90 • **Creative methodology.** First, the QFSTS model is the first on introducing the multivariate asymmetric Laplace (MAL) distribution to time series analysis. The idea of Bayesian quantile regression employing a likelihood function that is based on the asymmetric Laplace (AL) distribution, was introduced in the classical work by Yu and Moyeed (2001). The use of  
95 the AL distribution is proved as a very natural and effective way of modeling Bayesian quantile regression, irrespective of the original distribution of the data (Chen et al. (2013)). In Section 2.2, we rigorously establish the explicit linkage between the MAL distribution and joint quantile regression, by setting the specific forms of parameters of the MAL distributed  
100 error term.

Second, the QFSTS model achieves feature selection in joint quantile time series analysis. It is very challenging to conduct feature selection on correlated time series where each has its own predictors, while when it comes to select features in quantile regression, it is much more challenging in  
105 that one has to take quantiles into consideration instead of the mean. Further, the Bayesian quantile regression coefficients depend on the quantile of interest (Yu and Moyeed (2001)). That is, for different quantiles, the coefficient of any predictor varies. The QFSTS model creatively uses the Gibbs sampler for quantile feature selection by means of the classical “spike-and-slab” prior setup (George and McCulloch (1997); Madigan  
110 and Raftery (1994)), and the Metropolis-Hastings algorithm in drawing the MAL distributed error term.

Third, the QFSTS model introduces the Bayesian model averaging technique (Hoeting et al. (1999)) in joint quantile time series analysis. Consistent with the model training in the Bayesian paradigm, Bayesian model  
115

averaging provides a coherent mechanism to handle model uncertainty, by averaging the predicted quantile values from all the models generated in model training. In this way, we commit neither to any particular set of predictors which helps avoid an arbitrary selection, nor to point estimates of their coefficients which prevents overfitting.

120

- **Excellent performance.** Under the challenging situation that each time series has its own pool of predictors made of both continuous and categorical covariates (Papaxanthos et al. (2016)), the QFSTS model provides very accurate feature selection and parameter estimation results, thoroughly examined on simulated data, with different quantile values, different size of datasets, and different correlation values among multivariate time series. Extensive analyses on simulated data and empirical data confirmed that the QFSTS model outperforms the “auto.arima” function in ten steps of one-step ahead forecast consistently. The “auto.arima” function automatically fits the autoregressive integrated moving average with regression (ARIMAX) model that is the most classical and popular time series model.

125

- **Wide applicability.** First, because of the feature selection function embedded in the QFSTS model, it is applicable in proper applications that desire higher learning accuracy, lower computational cost, better model interpretability, and other benefits generated by feature selection. Second, different from most machine learning algorithms, because of the Bayesian paradigm embedded in the QFSTS model, it is applicable in proper applications that require Bayesian inference and learning. Third, because of the QFSTS model’s general model structure, it is applicable in more applications besides the finance applications demonstrated in this paper. At last, the QFSTS model requires small datasets to train, converges fast, and is executable on ordinary personal computers.

130

135

140

### 1.3. Organization of the paper

145 The rest of the paper proceeds as follows: In Section 2, we introduce the QFSTS model through explaining its model structure and then illustrating the linkage between the specific design of the QFSTS model with multivariate quantile prediction. In Section 3, we explain the methodology of the QFSTS model, by firstly write the system in the distribution equivalence matrix form, and  
150 then provide the prior setup and posterior formulas. In Section 4, we provide the model training algorithm and the joint quantile time series forecast algorithm. In Section 5, we demonstrate the model performance with simulated data generated by a three-dimensional target time series, and fully examine the QFSTS model's ability in selecting the correct variables, accuracy in parameter  
155 estimation, and strength in forecast, with different quantiles and time series correlations. In Section 6, we demonstrate the model performance with empirical daily stock price changes data of a stock portfolio including Bank of America, Capital One Financial Corporation, JPMorgan Chase & Company, and Wells Fargo & Company. In Section 7, we conclude and remark.

## 160 2. The QFSTS model

In this section, we introduce the QFSTS model, by firstly explaining its model structure in Section 2.1, and then illustrating the linkage between the specific design of the QFSTS model with multivariate quantile prediction in Section 2.2.

### 165 2.1. Model Structure

The QFSTS model is a structural time series model, which is constructed by components with direct interpretations, as follows:

$$\tilde{y}_t = \tilde{\mu}_t + \tilde{\xi}_t + \tilde{\epsilon}_t, \quad (1)$$

where  $t$  stands for a specific time point in  $\{1, \dots, n\}$ , the  $m$ -dimensional vector  $\tilde{y}_t$  represents target time series, the  $m$ -dimensional vector  $\tilde{\mu}_t$  represents the

linear trend component, the  $m$ -dimensional vector  $\tilde{\xi}_t$  represents the regression component, and the  $m$ -dimensional vector  $\tilde{\epsilon}_t$  represents the observation error term. Since structural time series models belong to state space models, the QFSTS model then belongs to state space models. In the following, we illustrate each time series components:

- The linear trend component  $\tilde{\mu}_t = [\mu_t^{(1)}, \dots, \mu_t^{(m)}]^T$  of the QFSTS model is a generalization of the local linear trend model, in the following form:

$$\mu_{t+1}^{(i)} = \mu_t^{(i)} + \delta_t^{(i)} + u_t^{(i)}, \quad [u_t^{(1)}, \dots, u_t^{(m)}]^T \stackrel{iid}{\sim} N_m(0, \Sigma_{\tilde{\mu}}), \quad (2)$$

$$\delta_{t+1}^{(i)} = D_i + \lambda_i(\delta_t^{(i)} - D_i) + v_t^{(i)}, \quad [v_t^{(1)}, \dots, v_t^{(m)}]^T \stackrel{iid}{\sim} N_m(0, \Sigma_{\tilde{\delta}}). \quad (3)$$

The QFSTS model allows each target series to have its own specific linear trend component. Here, for the  $i$ -th target series where  $i \in \{1, \dots, m\}$ ,  $\mu_t^{(i)}$  models the current “level” of the trend;  $\delta_t^{(i)}$  models the current “slope” of the trend which is the expected increase in  $\mu_t^{(i)}$  between time point  $t$  and time point  $t+1$ ; the parameter  $D_i$  models the “mean reversion” effect, i.e., a dynamic can be very unstable in the short run but stable in the long run; the parameter  $\lambda_i \in [0, 1]$  is the learning rate at which the local trend is updated.

- The regression component  $\tilde{\xi}_t = [\xi_t^{(1)}, \dots, \xi_t^{(m)}]^T$  of the QFSTS model is written as follows:

$$\xi_t^{(i)} = \beta_i^T x_t^{(i)}. \quad (4)$$

The QFSTS model allows each target series to have its own specific regression component. Here for  $i \in \{1, \dots, m\}$ ,  $x_t^{(i)} = [x_{t1}^{(i)}, \dots, x_{tk_i}^{(i)}]^T$  is the pool of all available  $k_i$  predictors at time  $t$  for the  $i$ -th target series, for example  $k_i = 30$  for the  $i$ -th target series and  $k_j = 20$  for the  $j$ -th target series where  $j \neq i$ ;  $\beta_i = [\beta_{i1}, \dots, \beta_{ik_i}]^T$  represents corresponding static regression coefficients for the  $i$ -th target series.



- The vector of observation error terms  $\tilde{\epsilon}_t = [\epsilon_t^{(1)}, \dots, \epsilon_t^{(m)}]^T$  follows the multivariate asymmetric Laplace (MAL) distribution

$$\tilde{\epsilon}_t \stackrel{iid}{\sim} \mathcal{AL}_m(\phi_\epsilon, \Sigma_\epsilon), \quad (5)$$

where  $\phi_\epsilon$  is a  $m$ -dimensional vector of means for each variable, and  $\Sigma_\epsilon$  is a  $m \times m$ -dimensional non-negative definite symmetric matrix of variance-covariance. When  $\phi_\epsilon = 0$ , the distribution  $\mathcal{AL}_m(0, \Sigma_\epsilon)$  is the symmetric multivariate Laplace distribution. We refer interested readers to Section 6.2 of Kotz et al. (2012) for further explanations of the MAL distribution.

## 2.2. The MAL Distribution and Joint Quantile Regression

In this section, we establish the linkage between the MAL distribution and joint quantile regression, by setting the specific forms of  $\phi_\epsilon$  and  $\Sigma_\epsilon$  in the  $\mathcal{AL}_m(\phi_\epsilon, \Sigma_\epsilon)$  distribution, which is given in equation (14).

Firstly, we subtract the trend time series component from the multivariate target time series and denote

$$\tilde{z}_t = [z_t^{(1)}, \dots, z_t^{(m)}]^T = \tilde{y}_t - \tilde{\mu}_t.$$

Then equation (1) becomes

$$\tilde{z}_t = \tilde{\xi}_t + \tilde{\epsilon}_t, \quad \tilde{\epsilon}_t \stackrel{iid}{\sim} \mathcal{AL}_m(\phi_\epsilon, \Sigma_\epsilon). \quad (6)$$

By Theorem 6.3.1 in Section 6.3 of Kotz et al. (2012),  $\tilde{\epsilon}_t$  can be represented as follows, in the distribution equivalence sense,

$$\tilde{\epsilon}_t = \phi_\epsilon W + W^{1/2} \tilde{e}_t, \quad W \stackrel{iid}{\sim} \text{Exp}(1), \quad \tilde{e}_t = [e_t^{(1)}, \dots, e_t^{(m)}]^T \stackrel{iid}{\sim} \mathcal{N}_m(0, \Sigma_\epsilon), \quad (7)$$

where  $W$  and  $\tilde{e}_t$  are independent, therefore we can rewrite (6) as

$$\tilde{z}_t = \tilde{\xi}_t + \phi_\epsilon W + W^{1/2} \tilde{e}_t, \quad (8)$$

in the distribution equivalence sense.

The specific forms of  $\phi_\epsilon$  and  $\Sigma_\epsilon$  in the  $\mathcal{AL}_m(\phi_\epsilon, \Sigma_\epsilon)$  distribution which link the MAL distribution with joint quantile regression, is based on the corresponding theory in the univariate case. Now, we summarize some of the findings in Yu and Moyeed (2001). The standard linear regression model is given by

$$y_t^u = (\mathbf{x}_t)^T \boldsymbol{\beta} + \epsilon_t^u,$$

where the superscript “ $u$ ” indicates the univariate case and bold symbols represent vectors. Here,  $\mathbf{x}_t$  is the vector of regressors;  $\boldsymbol{\beta}$  is the vector of corresponding coefficients; the error term  $\epsilon_t^u$  has zero mean and finite constant variance, but it is not necessary to specify its distribution as it can take any form. Suppose that the  $p$ -th ( $0 < p < 1$ ) quantile of the error term  $\epsilon_t^u$  is the value  $q_p$ , such that  $\mathbb{P}(\epsilon_t^u < q_p) = p$ . The  $p$ -th conditional quantile of  $y_t^u$  given  $\mathbf{x}_t$  is then simply

$$q_p(y_t^u | \mathbf{x}_t) = (\mathbf{x}_t)^T \boldsymbol{\beta}_p, \quad (9)$$

where  $\boldsymbol{\beta}_p$  is a vector of coefficients dependent on  $p$ .

The  $p$ -th regression quantile is defined as the solution  $\widehat{\boldsymbol{\beta}}_p$  to the quantile regression minimization problem

$$\min_{\boldsymbol{\beta}} \sum_t \rho_p \left( y_t^u - (\mathbf{x}_t)^T \boldsymbol{\beta} \right),$$

where  $\rho_p(\cdot)$  is a loss function that has robust properties (see, Huber (2004)) given by

$$\rho_p(u) = \frac{|u| + (2p - 1)u}{2}. \quad (10)$$

Yu and Moyeed (2001) showed that the minimization of the above loss function is exactly equivalent to the maximization of a likelihood function formed by combining independently distributed asymmetric Laplace (AL) densities, and the univariate AL distribution provides a direct connection between the quantile regression minimization problem and the maximum likelihood estimation.

A random variable  $U$  is said to follow the univariate AL distribution  $\mathcal{AL}(\theta_{\text{loc}}, \theta_{\text{sca}}, p)$  if its probability density function is given by

$$f_p(u) = \frac{p(1-p)}{\theta_{\text{sca}}} \exp \left\{ \rho_p \left( \frac{u - \theta_{\text{loc}}}{\theta_{\text{sca}}} \right) \right\},$$

where  $\rho_p(\cdot)$  is given in (10),  $\theta_{\text{loc}}$  is the location parameter, and  $\theta_{\text{sca}}$  is the scale parameter. The mean and the variance of  $U$  are given by

$$\mathbb{E}(U) = \theta_{\text{loc}} + \theta_{\text{sca}} \frac{2p-1}{p(1-p)}, \quad \text{Var}(U) = \theta_{\text{sca}}^2 \frac{1-2p+2p^2}{p^2(1-p)^2}.$$

Now we get back to equation (8) and investigate its univariate case of the  $i$ -th target series for  $i \in \{1, 2, \dots, m\}$ :

$$z_t^{(i)} = \xi_t^{(i)} + \phi_\epsilon^{(i)} W + W^{1/2} e_t^{(i)}, \quad e_t^{(i)} \stackrel{iid}{\sim} \mathcal{N}(0, (\Sigma_\epsilon)_{ii}), \quad (11)$$

Suppose we are interested in the  $\tau_i$ -th ( $0 < \tau_i < 1$ ) quantile and then we need  $z_t^{(i)}$  to satisfy the univariate AL distribution  $\mathcal{AL}(\xi_t^{(i)}, \phi_i^*, \tau_i)$ .

In order to obtain

$$\mathbb{E}(z_t^{(i)}) = \xi_t^{(i)} + \phi_i^* \frac{2\tau_i - 1}{\tau_i(1 - \tau_i)},$$

it suffices to set

$$\phi_\epsilon^{(i)} = \phi_i^* \frac{2\tau_i - 1}{\tau_i(1 - \tau_i)} \quad (12)$$

since

$$\mathbb{E}(\phi_\epsilon^{(i)} W) = \phi_\epsilon^{(i)} \quad \text{and} \quad \mathbb{E}(W^{1/2} e_t^{(i)}) = 0.$$

Furthermore, in order to obtain

$$\text{Var}(z_t^{(i)}) = (\phi_i^*)^2 \frac{1 - 2\tau_i + 2\tau_i^2}{\tau_i(1 - \tau_i)},$$

it suffices to set

$$(\Sigma_\epsilon)_{ii} = (\phi_i^*)^2 \frac{2}{\tau_i(1 - \tau_i)}, \quad (13)$$

since then

$$\begin{aligned} \text{Var}(z_t^{(i)}) &= \text{Var}(\phi_\epsilon^{(i)} W + W^{1/2} e_t^{(i)}) \\ &= \left( \phi_i^* \frac{2\tau_i - 1}{\tau_i(1 - \tau_i)} \right)^2 + (\phi_i^*)^2 \frac{2}{\tau_i(1 - \tau_i)} \\ &= (\phi_i^*)^2 \frac{1 - 2\tau_i + 2\tau_i^2}{\tau_i(1 - \tau_i)}. \end{aligned}$$

At last, in order to meet the univariate requirements (12) and (13), we can take

$$\phi_\epsilon = \Phi \tilde{\phi}_\tau \quad \text{and} \quad \Sigma_\epsilon = \Phi \Sigma_\tau \Phi = \Phi (\Psi_\tau \Sigma_{\text{corr}} \Psi_\tau) \Phi, \quad (14)$$

where  $\tilde{\phi}_\tau = \left[ \frac{2\tau_1-1}{\tau_1(1-\tau_1)}, \frac{2\tau_2-1}{\tau_2(1-\tau_2)}, \dots, \frac{2\tau_m-1}{\tau_m(1-\tau_m)} \right]^T$ ,  $\Sigma_{\text{corr}}$  is the correlation matrix,

$$\Phi = \begin{bmatrix} \phi_1 & 0 & \dots & 0 \\ 0 & \phi_2 & \dots & 0 \\ \vdots & \vdots & \ddots & \vdots \\ 0 & 0 & \dots & \phi_m \end{bmatrix}, \quad \Psi_\tau = \begin{bmatrix} \sqrt{\frac{2}{\tau_1(1-\tau_1)}} & 0 & \dots & 0 \\ 0 & \sqrt{\frac{2}{\tau_2(1-\tau_2)}} & \dots & 0 \\ \vdots & \vdots & \ddots & \vdots \\ 0 & 0 & \dots & \sqrt{\frac{2}{\tau_m(1-\tau_m)}} \end{bmatrix}.$$

### 205 3. Methodology

In this section, we explain the methodology of the QFSTS model. In Section 3.1, we write the system in the distribution equivalence matrix form to facilitate derivations following. In Section 3.2, we provide the prior setups including the “spike-and-slab” for variable selection in this Bayesian paradigm. In Section 210 3.3, we derive all necessary conditional probabilities, in order to implement the classical Gibbs sampler in model training.

#### 3.1. The Distribution Equivalence Matrix Form

Recall that by equations (8) we have

$$\tilde{z}_t = \tilde{\xi}_t + \phi_\epsilon W + W^{1/2} \tilde{e}_t.$$

Here,  $\tilde{z}_t = [z_t^{(1)}, \dots, z_t^{(m)}]^T$  is the  $m$ -dimensional vector generated by subtracting the trend time series component from the multivariate target time series;  $\tilde{\xi}_t = [\xi_t^{(1)}, \dots, \xi_t^{(m)}]^T$  is the  $m$ -dimensional regression component such that 215  $\xi_t^{(i)} = \beta_i^T x_t^{(i)}$ , where  $\beta_i = [\beta_{i,1}, \dots, \beta_{i,k_i}]^T$  is the collection of regression coefficients for the  $i$ -th response variable, and  $x_t^{(i)} = [x_{t1}^{(i)}, \dots, x_{tk_i}^{(i)}]^T$  is the pool of all available  $k_i$  predictors at time  $t$  for the  $i$ -th target series;  $\phi_\epsilon$  is the  $m$ -dimensional vector of means for the  $m$ -dimensional error term.

Now, we define the  $n \times m$  matrix  $Z$  as

$$Z = [\tilde{z}_1, \dots, \tilde{z}_n]^T = \left[ \begin{array}{c} \left[ \begin{array}{c} z_1^{(1)} \\ \vdots \\ z_n^{(1)} \end{array} \right], \dots, \left[ \begin{array}{c} z_n^{(1)} \\ \vdots \\ z_n^{(m)} \end{array} \right] \end{array} \right]^T = \left[ \begin{array}{ccc} \left[ \begin{array}{c} z_1^{(1)} \\ \vdots \\ z_n^{(1)} \end{array} \right] & \dots & \left[ \begin{array}{c} z_1^{(m)} \\ \vdots \\ z_n^{(m)} \end{array} \right] \end{array} \right]^T,$$

and then define the  $mn$ -dimensional vector  $\tilde{Z}$  as

$$\tilde{Z} = \text{vec}(Z) = \left[ \left[ \begin{array}{ccc} z_1^{(1)} & \dots & z_n^{(1)} \end{array} \right], \dots, \left[ \begin{array}{ccc} z_1^{(m)} & \dots & z_n^{(m)} \end{array} \right] \right]^T.$$

Analogously, we define the  $mn$ -dimensional vector  $\tilde{E}$  as

$$\tilde{E} = \text{vec}(E) \quad \text{where} \quad E = [\tilde{\epsilon}_1, \dots, \tilde{\epsilon}_n]^T,$$

and define the  $mn$ -dimensional vector  $\tilde{\Phi}_\epsilon$  as

$$\tilde{\Phi}_\epsilon = \text{vec}(\Phi_\epsilon) \quad \text{where} \quad \Phi_\epsilon = [\phi_\epsilon, \dots, \phi_\epsilon]^T.$$

Define  $\beta$  as the  $K$ -dimensional ( $K = \sum_{i=1}^m k_i$ ) vector of regression coefficients

$$\beta = [\beta_1^T, \dots, \beta_m^T]^T \quad \text{where} \quad \beta_i = [\beta_{i,1}, \dots, \beta_{i,k_i}]^T.$$

Define  $X_i$  as the  $n \times k_i$  matrix representing all observations of  $k_i$  possible predictors for the  $i$ -th response variable

$$X_i = \left[ (x_1^{(i)})^T, \dots, (x_n^{(i)})^T \right]^T = \begin{bmatrix} x_{1,1}^{(i)} & x_{1,2}^{(i)} & x_{1,3}^{(i)} & \dots & x_{1,k_i}^{(i)} \\ x_{2,1}^{(i)} & x_{2,2}^{(i)} & x_{2,i,3}^{(i)} & \dots & x_{2,k_i}^{(i)} \\ \vdots & \vdots & \vdots & \ddots & \vdots \\ x_{n,1}^{(i)} & x_{n,2}^{(i)} & x_{n,3}^{(i)} & \dots & x_{n,k_i}^{(i)} \end{bmatrix}, \quad (15)$$

and further define  $X$  as the  $mn \times K$ -dimensional predictor matrix

$$X = \begin{bmatrix} X_1 & 0 & 0 & \dots & 0 \\ 0 & X_2 & 0 & \dots & 0 \\ \vdots & \vdots & \vdots & \ddots & \vdots \\ 0 & 0 & 0 & \dots & X_m \end{bmatrix}. \quad (16)$$

Then we have the following expression, in the distribution equivalence sense,

$$\tilde{Z} = X\beta + \tilde{\Phi}_\epsilon W + W^{1/2} \tilde{E}. \quad (17)$$

The “spike-and-slab” prior setup is a Bayesian variable selection technique, where the “spike” is the probability of a particular coefficient in the model to be zero, and the “slab” is the prior distribution for the regression coefficient values. To specify “spike” prior, a vector of  $K = \sum_{i=1}^m k_i$  indicator variables

$$\gamma = [\gamma_{1,1}, \dots, \gamma_{1,k_1}, \gamma_{2,1}, \dots, \gamma_{2,k_2}, \dots, \gamma_{m,1}, \dots, \gamma_{m,k_m}]$$

is introduced according to the rule:

$$\gamma_{i,k} = \begin{cases} 1 & \text{if } \beta_{i,k} \neq 0, \\ 0 & \text{otherwise.} \end{cases}$$

Regressor indicators are assumed to be independent Bernoulli variables:

$$p(\gamma|W) = \prod_{i=1}^m \prod_{k=1}^{k_i} \pi_{i,k}^{\gamma_{i,k}} (1 - \pi_{i,k})^{1-\gamma_{i,k}}, \quad 0 \leq \pi_{i,k} = p(\gamma_{i,k}) \leq 1, \quad (18)$$

where  $\pi_{i,k}$  is the prior inclusion probability. Equation (18) is often simplified by setting  $\pi_{i,k} = \pi_i$ , if prior information of specific predictors on response variables is not available. One could further simplify by setting  $\pi_i = q_i/k_i$ , where  $k_i$  is the total number of candidate predictors for the  $i$ -th target series and  $q_i$  is the total number of nonzero expected predictors given by researchers. When there is sufficient prior information, assigning subjectively determined values to  $\pi_{i,k}$  might provide more robust results. One could also force certain variables to be excluded or included by setting  $\pi_{ij}$  as 0 or 1. By default and in all the experimental examinations following, we set  $\pi_{ik} = 0.5$  for all  $i \in \{1, \dots, m\}$  and all  $k \in \{1, \dots, k_i\}$ .

We use a simple conventional prior specification which makes  $\beta$  and  $\Sigma_\epsilon$  conditionally independent

$$p(\beta, \Sigma_\tau | \gamma, \Phi, W) = p(\beta | \gamma, \Phi, W) \times p(\Sigma_\tau | \gamma, \Phi, W), \quad (19)$$

where

$$\beta | \gamma, \Phi, W \stackrel{iid}{\sim} N_K(b_\gamma, A_\gamma^{-1}), \quad \Sigma_\tau | \gamma, \Phi, W \stackrel{iid}{\sim} IW_m(v_0, V_0). \quad (20)$$

Equation (20) is the “slab” prior because, conditional on  $\gamma$ , one can choose the prior parameters to make it only very weakly informative and close to flat.  $N_K(b_\gamma, A_\gamma^{-1})$  stands for the  $K$ -dimensional multivariate normal distribution,  $b_\gamma$  is the vector of prior means, and  $A_\gamma$  is the full-model prior information matrix. One can set  $A_\gamma = \kappa X_\gamma^T X_\gamma / n$  where  $\kappa$  is the number of observations worth of weight on the prior mean vector  $b_\gamma$ .  $IW_m(v_0, V_0)$  stands for the  $m$ -dimensional inverse Wishart distribution, where  $v_0$  is the number of degrees of freedom and  $V_0$  is a  $m \times m$  scale matrix. One can ask analysts for an expected  $R^2$ , and a number of observations worth of weight  $v_0$  which must be greater than the dimension of  $\tilde{y}_t$  plus one, and set

$$V_0 = (v_0 - m - 1)(1 - R^2)\Sigma_y,$$

230 where  $\Sigma_y$  is the variance-covariance matrix for multiple target time series. By default and in all the experimental examinations following, we set  $b_\gamma = 0$ ,  $\kappa = 0.01$ ,  $R^2 = 0.8$ , and  $v_0 = 5$ .

To simplify the derivation of  $\Phi$ 's posterior distribution, we set the prior distribution of  $\Phi$  as

$$\Phi \sim \delta(\Phi_0) \tag{21}$$

where  $\delta(\cdot)$  is the Dirac delta function. That is, the initial value of  $\Phi$  is deterministic with value  $\Phi_0$ . In the implement of the QFSTS model, one can  
 235 give user-desired initial values of  $\Phi$  or tune  $\Phi_0$  based on model training results. Recall that  $\Phi$  is defined as diagonal in (14), hence there are only  $m$  hyper-parameters of  $\Phi$  for  $m$  target time series. The default value of  $\Phi_0$  is a diagonal matrix with values 0.1 on the diagonal. As in any Markov chain analysis, better tuned initial values yield fast convergences which would save  
 240 great MCMC efforts. In the numerical examinations with simulated data, we set  $\Phi_0 = \text{diag}(0.7, 0.6, 0.9)$ ; in the numerical examinations with empirical data, we set  $\Phi_0 = \text{diag}(0.01, 0.00005, 0.05, 0.005)$ , where  $\text{diag}(A)$  creates a diagonal matrix with diagonal entries taking values in the order of the vector  $A$ .

The prior distributions of variance-covariance matrices in the trend compo-

ment are set as inverse Wishart distributed

$$\Sigma_\alpha \stackrel{iid}{\sim} IW_m(\nu_\alpha, V_\alpha), \quad \alpha \in \{\tilde{\mu}, \tilde{\delta}\}. \quad (22)$$

By default and in all the experimental examinations following, we set  $\nu_\alpha = V_\alpha =$   
 245 0.01.

### 3.3. Posterior Conditional Distributions

In order to implement the classical Gibbs sampler in this multivariate setting, we derive all necessary conditional probabilities of  $\tilde{Z}$ ,  $\beta$ ,  $\Phi$ ,  $\Sigma_\tau$ ,  $\gamma$ , and  $W$ . The full likelihood function is given by

$$p(\tilde{Z}, \beta, \Phi, \Sigma_\tau, \gamma, W) = p(\tilde{Z}|\beta, \Phi, \Sigma_\tau, \gamma, W) \times p(\beta, \Phi, \Sigma_\tau, |\gamma, W) \times p(\gamma|W) \times p(W).$$

Then, by equations (17), (18), (19), (20), and (21), we have that

$$\begin{aligned} & p(\tilde{Z}, \beta, \Phi, \Sigma_\tau, \gamma, W) \\ & \propto p(\tilde{Z}|\beta, \Phi, \Sigma_\tau, \gamma, W) \times p(\beta|\gamma, W) \times p(\Sigma_\tau|\gamma, W) \times p(\gamma|W) \times p(W) \\ & \propto |W\Phi\Sigma_\tau\Phi|^{-n/2} \exp\left(-\frac{1}{2W}(\tilde{Z} - X_\gamma\beta_\gamma - \tilde{\Phi}_\epsilon W)^T((\Phi\Sigma_\tau\Phi)^{-1} \otimes I_n)(\tilde{Z} - X_\gamma\beta_\gamma - \tilde{\Phi}_\epsilon W)\right) \\ & \quad \times |A_\gamma|^{1/2} \exp\left(-\frac{1}{2}(\beta_\gamma - b_\gamma)^T A_\gamma(\beta_\gamma - b_\gamma)\right) |\Sigma_\tau|^{-(v_0+m+1)/2} \exp\left(-\frac{1}{2}\text{tr}(V_0\Sigma_\tau^{-1})\right) \\ & \quad \times p(\gamma|W) \times p(W), \end{aligned} \quad (23)$$

where  $|\cdot|$  stands for the determinant of a matrix,  $\otimes$  is the Kronecker product, and  $\text{tr}(\cdot)$  represents the trace of a matrix.

#### 3.3.1. Posterior Conditional Distribution of $\beta$

To facilitate derivation, we firstly transform

$$\tilde{Z} = X\beta + \tilde{\Phi}_\epsilon W + W^{1/2}\tilde{E},$$

where

$$\tilde{E} = \text{vec}(E) = \text{vec}([\tilde{\epsilon}_1, \dots, \tilde{\epsilon}_n]^T), \quad \tilde{\epsilon}_t \stackrel{iid}{\sim} \mathcal{N}_m(0, \Sigma_\epsilon = \Phi\Sigma_\tau\Phi),$$



to a system with uncorrelated errors using the Cholesky decomposition of  $\Sigma_\tau$ ,

$$\Sigma_\tau = U^T U, \quad \text{i.e. } (U^{-1})^T \Sigma_\tau U^{-1} = I. \quad (24)$$

Thus we have the transformed system with uncorrelated errors:

$$\widehat{Z} = \widehat{X}\beta + \widehat{\Phi}_\epsilon W + W^{1/2}\widehat{E}, \quad (25)$$

where

$$\begin{aligned} \widehat{Z} &= (((U\Phi)^{-1})^T \otimes I_n) \widetilde{Z}, & \widehat{X} &= (((U\Phi)^{-1})^T \otimes I_n) X, \\ \widehat{\Phi}_\epsilon &= (((U\Phi)^{-1})^T \otimes I_n) \widetilde{\Phi}_\epsilon, & \widehat{E} &= (((U\Phi)^{-1})^T \otimes I_n) \widetilde{E}. \end{aligned} \quad (26)$$

For the following term in the first exponential in (23), we have

$$\begin{aligned} & (\widetilde{Z} - X_\gamma \beta_\gamma - \widetilde{\Phi}_\epsilon W)^T ((\Phi \Sigma_\tau \Phi)^{-1} \otimes I_n) (\widetilde{Z} - X_\gamma \beta_\gamma - \widetilde{\Phi}_\epsilon W) \\ &= (\widetilde{Z} - X_\gamma \beta_\gamma - \widetilde{\Phi}_\epsilon W)^T (([U\Phi]^T U\Phi)^{-1} \otimes I_n) (\widetilde{Z} - X_\gamma \beta_\gamma - \widetilde{\Phi}_\epsilon W) \\ &= (\widetilde{Z} - X_\gamma \beta_\gamma - \widetilde{\Phi}_\epsilon W)^T ((U\Phi)^{-1} \otimes I_n) \times (((U\Phi)^{-1})^T \otimes I_n) (\widetilde{Z} - X_\gamma \beta_\gamma - \widetilde{\Phi}_\epsilon W) \\ &= (\widehat{Z} - \widehat{X}_\gamma \beta_\gamma - \widehat{\Phi}_\epsilon W)^T (\widehat{Z} - \widehat{X}_\gamma \beta_\gamma - \widehat{\Phi}_\epsilon W). \end{aligned} \quad (27)$$

The full conditional distribution of  $\beta$  can be expressed as:

$$\begin{aligned} p(\beta | \widehat{Z}, \Phi, \Sigma_\epsilon, \gamma, W) &\propto \exp\left(-\frac{1}{2} W^{-1} (\widehat{Z} - \widehat{X}_\gamma \beta_\gamma - \widehat{\Phi}_\epsilon W)^T (\widehat{Z} - \widehat{X}_\gamma \beta_\gamma - \widehat{\Phi}_\epsilon W)\right) \\ &\quad \times \exp\left(-\frac{1}{2} (\beta_\gamma - b_\gamma)^T A_\gamma (\beta_\gamma - b_\gamma)\right). \end{aligned}$$

Terms in the above exponential can be written as

$$\begin{aligned} & W^{-1} (\widehat{Z} - \widehat{X}_\gamma \beta_\gamma - \widehat{\Phi}_\epsilon W)^T (\widehat{Z} - \widehat{X}_\gamma \beta_\gamma - \widehat{\Phi}_\epsilon W) + (\beta_\gamma - b_\gamma)^T A_\gamma (\beta_\gamma - b_\gamma) \\ &= \beta_\gamma^T (W^{-1} \widehat{X}_\gamma^T \widehat{X}_\gamma + A_\gamma) \beta_\gamma - \beta_\gamma^T (W^{-1} \widehat{X}_\gamma^T \widehat{Z} - \widehat{X}_\gamma^T \widehat{\Phi}_\epsilon + A_\gamma b_\gamma) \\ &\quad - (W^{-1} \widehat{X}_\gamma^T \widehat{Z} - \widehat{X}_\gamma^T \widehat{\Phi}_\epsilon + A_\gamma b_\gamma)^T \beta_\gamma + W^{-1} (\widehat{Z} - \widehat{\Phi}_\epsilon W)^T (\widehat{Z} - \widehat{\Phi}_\epsilon W) + b_\gamma^T A_\gamma b_\gamma \\ &= (\beta_\gamma - \bar{\beta}_\gamma)^T (W^{-1} \widehat{X}_\gamma^T \widehat{X}_\gamma + A_\gamma) (\beta_\gamma - \bar{\beta}_\gamma) + W^{-1} (\widehat{Z} - \widehat{\Phi}_\epsilon W)^T (\widehat{Z} - \widehat{\Phi}_\epsilon W) \\ &\quad + b_\gamma^T A_\gamma b_\gamma - (\bar{\beta}_\gamma)^T (W^{-1} \widehat{X}_\gamma^T \widehat{X}_\gamma + A_\gamma) \bar{\beta}_\gamma, \end{aligned} \quad (28)$$

where

$$\bar{\beta}_\gamma = (W^{-1} \widehat{X}_\gamma^T \widehat{X}_\gamma + A_\gamma)^{-1} (W^{-1} \widehat{X}_\gamma^T \widehat{Z} - \widehat{X}_\gamma^T \widehat{\Phi}_\epsilon + A_\gamma b_\gamma).$$

Therefore,  $\beta$  is still conditionally multivariate normal distributed

$$\beta|\widehat{Z}, \Phi, \Sigma_\tau, \gamma, W \stackrel{iid}{\sim} N_K(\bar{\beta}_\gamma, (W^{-1}\widehat{X}_\gamma^T\widehat{X}_\gamma + A_\gamma)^{-1}). \quad (29)$$

### 250 3.3.2. Posterior Conditional Distribution of $\Sigma_\tau$

Recalling that  $X_i$  is the  $n \times k_i$ -dimensional matrix given in equation (15), define the  $n \times K$ -dimensional ( $K = \sum_{i=1}^m k_i$ ) matrix  $X_\gamma^*$  as

$$X_\gamma^* = [X_1, X_2, \dots, X_m]_\gamma.$$

Define the  $K \times m$ -dimensional matrix  $B_\gamma$  as

$$B_\gamma = \begin{bmatrix} \beta_1 & 0 & 0 & \dots & 0 \\ 0 & \beta_2 & 0 & \dots & 0 \\ \vdots & \vdots & \vdots & \ddots & \vdots \\ 0 & 0 & 0 & \dots & \beta_m \end{bmatrix}_\gamma, \quad \beta_i = \begin{bmatrix} \beta_{i,1} \\ \vdots \\ \beta_{i,k_i} \end{bmatrix},$$

where  $\beta_i$  is the  $k_i$ -dimensional vector containing the collection of regression coefficients for the  $i$ -th response series. For the reason that trace is invariant under cyclic permutations, from equation (23), we know that

$$\begin{aligned} & (\widetilde{Z} - X_\gamma\beta_\gamma - \widetilde{\Phi}_\epsilon W)^T ((\Phi\Sigma_\tau\Phi) \otimes I_n)^{-1} (\widetilde{Z} - X_\gamma\beta_\gamma - \widetilde{\Phi}_\epsilon W) \\ &= \text{vec} \left( Z - X_\gamma^* B_\gamma - \Phi_\epsilon W \right)^T ((\Phi\Sigma_\tau\Phi)^{-1} \otimes I_n) \text{vec} \left( Z - X_\gamma^* B_\gamma - \Phi_\epsilon W \right) \\ &= \text{tr} \left( (Z - X_\gamma^* B_\gamma - \Phi_\epsilon W)^T (Z - X_\gamma^* B_\gamma - \Phi_\epsilon W) \Phi^{-1} \Sigma_\tau^{-1} \Phi^{-1} \right) \\ &= \text{tr} \left( \left[ (Z - X_\gamma^* B_\gamma - \Phi_\epsilon W) \Phi^{-1} \right] \Sigma_\tau^{-1} \left[ (Z - X_\gamma^* B_\gamma - \Phi_\epsilon W) \Phi^{-1} \right]^T \right) \\ &= \text{tr} \left( \left[ (Z - X_\gamma^* B_\gamma - \Phi_\epsilon W) \Phi^{-1} \right]^T \left[ (Z - X_\gamma^* B_\gamma - \Phi_\epsilon W) \Phi^{-1} \right] \Sigma_\tau^{-1} \right), \end{aligned}$$

and then we have

$$\begin{aligned} & p(\Sigma_\tau | \widetilde{Z}, \Phi, \beta, \gamma, W) \\ & \propto |\Sigma_\tau|^{-(n+v_0+m+1)/2} \exp \left( -\frac{1}{2} \text{tr} \left( \frac{1}{W} \left[ (Z - X_\gamma^* B_\gamma - \Phi_\epsilon W) \Phi^{-1} \right]^T \right. \right. \\ & \quad \left. \left. \times \left[ (Z - X_\gamma^* B_\gamma - \Phi_\epsilon W) \Phi^{-1} \right] \Sigma_\tau^{-1} + V_0 \Sigma_\tau^{-1} \right) \right). \end{aligned}$$

That is, the posterior conditional distribution of  $\Sigma_\tau$  is in the invert Wishart form

$$\begin{aligned} \Sigma_\tau | \tilde{Z}, \beta, \Phi, \gamma, W & \quad (30) \\ \stackrel{iid}{\sim} IW_m \left( v_0 + n, \frac{1}{W} \left[ (Z - X_\gamma^* B_\gamma - \Phi_\epsilon W) \Phi^{-1} \right]^T \left[ (Z - X_\gamma^* B_\gamma - \Phi_\epsilon W) \Phi^{-1} \right] + V_0 \right). \end{aligned}$$

### 3.3.3. Posterior Conditional Distribution of $\Phi$

Recall that by the Cholesky decomposition in (24) we have that  $\Sigma_\tau = U^T U$ . Further recall that by (14) we have that the  $m$ -dimensional vector  $\phi_\epsilon = \Phi \tilde{\phi}_\tau$  where  $\Phi$  is a  $m \times m$ -dimensional diagonal matrix and  $\tilde{\phi}_\tau$  is a  $m$ -dimensional vector, and then we can write the  $n \times m$ -dimensional matrix  $\Phi_\epsilon$  as

$$\Phi_\epsilon = [\phi_\epsilon, \dots, \phi_\epsilon]^T = \tilde{\Phi}_\tau \Phi, \quad \text{where} \quad \tilde{\Phi}_\tau = [\tilde{\phi}_\tau, \dots, \tilde{\phi}_\tau]^T.$$

Then by (23) we have

$$\begin{aligned} & p(\Phi | \tilde{Z}, \beta, \Sigma_\tau, \gamma, W) \\ & \propto |\Phi|^{-n} \exp \left( -\frac{1}{2} \text{tr} \left( \frac{1}{W} \left[ (Z - X_\gamma^* B_\gamma - \Phi_\epsilon W) \Phi^{-1} \right]^T \right. \right. \\ & \quad \left. \left. \times \left[ (Z - X_\gamma^* B_\gamma - \Phi_\epsilon W) \Phi^{-1} \right] \Sigma_\tau^{-1} \right) \right) \\ & \propto |\Phi|^{-n} \exp \left( -\frac{1}{2} \text{tr} \left( \frac{1}{W} \left[ (Z - X_\gamma^* B_\gamma - \Phi_\epsilon W) \Phi^{-1} \right]^T \right. \right. \\ & \quad \left. \left. \times \left[ (Z - X_\gamma^* B_\gamma - \Phi_\epsilon W) \Phi^{-1} \right] U^{-1} (U^{-1})^T \right) \right) \\ & \propto |\Phi|^{-n} \exp \left( -\frac{1}{2} \text{tr} \left( \frac{1}{W} \left[ (Z - X_\gamma^* B_\gamma - \Phi_\epsilon W) \Phi^{-1} U^{-1} \right]^T \right. \right. \\ & \quad \left. \left. \times \left[ (Z - X_\gamma^* B_\gamma - \Phi_\epsilon W) \Phi^{-1} U^{-1} \right] \right) \right) \\ & \propto |\Phi|^{-n} \exp \left( -\frac{1}{2} \text{tr} \left( \frac{1}{W} \left[ (Z - X_\gamma^* B_\gamma - \tilde{\Phi}_\tau \Phi W) \Phi^{-1} U^{-1} \right]^T \right. \right. \\ & \quad \left. \left. \times \left[ (Z - X_\gamma^* B_\gamma - \tilde{\Phi}_\tau \Phi W) \Phi^{-1} U^{-1} \right] \right) \right) \\ & \propto |\Phi|^{-n} \exp \left( -\frac{1}{2} \text{tr} \left( \frac{1}{W} \left[ (Z - X_\gamma^* B_\gamma) \Phi^{-1} U^{-1} - \tilde{\Phi}_\tau U^{-1} W \right]^T \right. \right. \end{aligned} \quad (31)$$

$$\times \left[ (Z - X_\gamma^* B_\gamma) \Phi^{-1} U^{-1} - \tilde{\Phi}_\tau U^{-1} W \right] \Big) \Big)$$

### 3.3.4. Posterior Conditional Distribution of $\gamma$

By equations (23) and (28), we know that

$$\begin{aligned} & p(\tilde{Z}, \beta, \Phi, \Sigma_\tau, \gamma, W) \\ & \propto \exp \left( -\frac{1}{2} \left[ (\beta - \bar{\beta}_\gamma)^T (W^{-1} \hat{X}_\gamma^T \hat{X}_\gamma + A_\gamma) (\beta - \bar{\beta}_\gamma) + W^{-1} (\hat{Z} - \hat{\Phi}_\epsilon W)^T (\hat{Z} - \hat{\Phi}_\epsilon W) \right] \right) \\ & \quad \times |A_\gamma|^{1/2} \exp \left( -\frac{1}{2} \left[ \text{tr}(V_0 \Sigma_\epsilon^{-1}) + b_\gamma^T A_\gamma b_\gamma - (\bar{\beta}_\gamma)^T (W^{-1} \hat{X}_\gamma^T \hat{X}_\gamma + A_\gamma) \bar{\beta}_\gamma \right] \right) p(\gamma|W) \\ & \quad \times |W \Phi \Sigma_\tau \Phi|^{-n/2} |\Sigma_\tau|^{-(v_0+m+1)/2} p(W), \end{aligned}$$

where

$$\bar{\beta}_\gamma = (W^{-1} \hat{X}_\gamma^T \hat{X}_\gamma + A_\gamma)^{-1} (W^{-1} \hat{X}_\gamma^T \hat{Z} - \hat{X}_\gamma^T \hat{\Phi}_\epsilon + A_\gamma b_\gamma).$$

Furthermore, by the fact that

$$\beta | \hat{Z}, \Phi, \Sigma_\tau, \gamma, W \stackrel{iid}{\sim} N_K(\bar{\beta}_\gamma, (W^{-1} \hat{X}_\gamma^T \hat{X}_\gamma + A_\gamma)^{-1}),$$

we have

$$\int_{-\infty}^{\infty} \exp \left( -\frac{1}{2} (\beta - \bar{\beta}_\gamma)^T (W^{-1} \hat{X}_\gamma^T \hat{X}_\gamma + A_\gamma) (\beta - \bar{\beta}_\gamma) \right) d\beta \propto (W^{-1} \hat{X}_\gamma^T \hat{X}_\gamma + A_\gamma)^{-1/2},$$

and then

$$\begin{aligned} & p(\tilde{Z}, \Phi, \Sigma_\tau, \gamma, W) \\ & = \int_{-\infty}^{\infty} p(\tilde{Z}, \beta, \Phi, \Sigma_\tau, \gamma, W) d\beta \\ & \propto \exp \left( -\frac{1}{2} \left[ W^{-1} (\hat{Z} - \hat{\Phi}_\epsilon W)^T (\hat{Z} - \hat{\Phi}_\epsilon W) - \Xi_\gamma^T (W^{-1} \hat{X}_\gamma^T \hat{X}_\gamma + A_\gamma)^{-1} \Xi_\gamma \right] \right) \\ & \quad \times |A_\gamma|^{1/2} \exp \left( -\frac{1}{2} \left[ \text{tr}(V_0 \Sigma_\epsilon^{-1}) + b_\gamma^T A_\gamma b_\gamma \right] \right) (W^{-1} \hat{X}_\gamma^T \hat{X}_\gamma + A_\gamma)^{-1/2} p(\gamma|W) \\ & \quad \times |W \Phi \Sigma_\tau \Phi|^{-n/2} |\Sigma_\tau|^{-(v_0+m+1)/2} p(W), \end{aligned}$$

where

$$\Xi_\gamma = (W^{-1} \hat{X}_\gamma^T \hat{Z} - \hat{X}_\gamma^T \hat{\Phi}_\epsilon + A_\gamma b_\gamma).$$

Therefore, the posterior conditional distribution of  $\gamma$  is given by

$$\begin{aligned} p(\gamma | \tilde{Z}, \Phi, \Sigma_\tau, W) & \propto \exp \left( -\frac{1}{2} \left[ b_\gamma^T A_\gamma b_\gamma - \Xi_\gamma^T (W^{-1} \hat{X}_\gamma^T \hat{X}_\gamma + A_\gamma)^{-1} \Xi_\gamma \right] \right) \\ & \quad \times |A_\gamma|^{1/2} (W^{-1} \hat{X}_\gamma^T \hat{X}_\gamma + A_\gamma)^{-1/2} p(\gamma|W). \end{aligned} \quad (32)$$

### 3.3.5. Posterior Conditional Distribution of $W$

Recall that the generalized inverse Gaussian distribution (GIG) is a three-parameter family of continuous probability distributions with probability density function (see page 1 of Jorgensen (2012))

$$f(x) = \frac{(a/b)^{p/2}}{2K_p(\sqrt{ab})} x^{(p-1)} e^{-(ax+b/x)/2}, \quad x > 0,$$

where  $K_p$  is a modified Bessel function of the second kind,  $a > 0$ ,  $b > 0$ , and  $p$  is a real parameter. By equations (23) and (27), we have that

$$p(W|\tilde{Z}, \beta, \tilde{\Phi}, \Sigma_\epsilon, \gamma) \propto |W|^{-n/2} \exp\left(-\frac{1}{2W}(\hat{Z} - \hat{X}_\gamma\beta_\gamma - \hat{\Phi}_\epsilon W)^T(\hat{Z} - \hat{X}_\gamma\beta_\gamma - \hat{\Phi}_\epsilon W) - W\right),$$

based on which,

$$W|\tilde{Z}, \beta, \Sigma_\epsilon, \gamma \stackrel{iid}{\sim} \text{GIG}(a, b, p), \quad (33)$$

$$a = 2 + \hat{\Phi}_\epsilon^T \hat{\Phi}_\epsilon, \quad b = (\hat{Z} - \hat{X}_\gamma\beta_\gamma)^T(\hat{Z} - \hat{X}_\gamma\beta_\gamma), \quad p = 1 - n/2.$$

### 3.3.6. Posterior Conditional Distribution of $\Sigma_\alpha$

Next we need to derive conditional posterior distribution of  $\Sigma_\alpha$  where  $\alpha \in \{\tilde{\mu}, \tilde{\delta}\}$  in the trend component. Similarly, as the posterior conditional distribution of  $\Sigma_\tau$  in the invert Wishart form in equation (30), the posterior distribution of  $\Sigma_\alpha$  is conditionally inverse Wishart distributed

$$\Sigma_\alpha|\tilde{Y}, \alpha, W \stackrel{iid}{\sim} IW_m\left(\nu_\alpha + n, V_\alpha + \frac{1}{W}AA^T\right), \quad \alpha \in \{\tilde{\mu}, \tilde{\delta}\}, \quad (34)$$

255 where  $A$  is the matrix of a collection of residues of each time series component.

## 4. Algorithms

Gibbs sampling is a Markov chain Monte Carlo (MCMC) algorithm for obtaining a sequence of observations, which are approximated from a specified multivariate probability distribution. MCMC methods are to construct a Markov chain that has the desired distribution as its equilibrium distribution. One can draw samples of the desired distribution by discarding the initial MCMC steps

260

as “burn-in”, since the quality of samples is an increasing function of the number of steps. In Algorithm 1, the posterior distributions of the model are simulated by Gibbs sampling approach, in the way that looping through the 7 steps yields a sequence of draws  $\theta = (\alpha, \Sigma_\alpha, \beta, \Phi, \Sigma_\tau, \gamma, W)$  where  $\alpha \in \{\tilde{\mu}, \tilde{\delta}\}$ , from a Markov chain with the stationary probability distribution  $p(\theta|Y)$  which is the posterior distribution of  $\theta$  given  $Y$ .

---

**Algorithm 1** Model Training

---

**Time series state components**

- 1: Draw the latent state  $\alpha$  from  $p(\alpha|\tilde{Y}, \Sigma_\alpha, \beta, \Phi, \Sigma_\tau, \gamma, W)$  where  $\alpha \in \{\tilde{\mu}, \tilde{\delta}\}$ , using the posterior simulation algorithm from Durbin and Koopman (2002).
- 2: Draw time series state component parameters  $\Sigma_\alpha$  from  $\Sigma_\alpha \stackrel{iid}{\sim} p(\Sigma_\alpha|\tilde{Y}, \alpha, W)$  based on the inverse Wishart distribution in equation (34).

**Quantile regression component**

- 3: Loop over  $i$  in an random order, draw each  $\gamma_i|\gamma_{-i}, \tilde{Z}, \Phi, \Sigma_\tau, W$ , namely simulating  $\gamma \stackrel{iid}{\sim} p(\gamma|\tilde{Z}, \Phi, \Sigma_\tau, W)$  in equation (32), using the stochastic search variable selection (SSVS) algorithm from George and McCulloch (1997).
- 4: Draw  $\beta$  from  $\beta \stackrel{iid}{\sim} p(\beta|\tilde{Z}, \Phi, \Sigma_\tau, \gamma, W)$  based on the multivariate normal distribution in equation (29).

**Error term**

- 5: Draw  $\Sigma_\tau$  from  $\Sigma_\tau \stackrel{iid}{\sim} p(\Sigma_\tau|\tilde{Z}, \beta, \Phi, \gamma, W)$  based on the inverse Wishart distribution in equation (30).
  - 6: Draw  $\Phi$  based on  $p(\Phi|\tilde{Z}, \beta, \Sigma_\tau, \gamma, W)$  in equation (31), using the Metropolis-Hastings Algorithms (see Chapter 6.3.1 of Robert and Casella (2010) and the references therein).
  - 7: Draw  $W$  from  $W \stackrel{iid}{\sim} p(W|\tilde{Z}, \beta, \Sigma_\tau, \gamma)$  based on the generalized inverse Gaussian distribution in equation (33).
- 

Given draws of model parameters and latent states from their posterior

---

**Algorithm 2** Joint Quantile Predictions

---

- 1: Draw the next trend component  $\alpha_{t+1} = (\tilde{\mu}_{t+1}, \tilde{\delta}_{t+1})$ , given current trend component  $\alpha_t = (\tilde{\mu}_t, \tilde{\delta}_t)$  and variance-covariance parameters  $\Sigma_\alpha = (\Sigma_{\tilde{\mu}}, \Sigma_{\tilde{\delta}})$ , by equations (2) and (3).
- 2: Based on indicator variable  $\gamma$ , compute the regression component  $\tilde{\xi}_{t+1}$  given the information about predictors at time  $t + 1$ , by equation (4).
- 3: Draw a random error  $\tilde{\epsilon}_{t+1}$  in the multivariate asymmetric Laplace distribution by equation (5), whose mean and variance are generated by expressions given in equation (14).
- 4: Sum up  $\tilde{\mu}_{t+1}$ ,  $\tilde{\xi}_{t+1}$ , and  $\tilde{\epsilon}_{t+1}$  to generate predictions, by equation (1).
- 5: Sum up all the generated predictions and divide by the total number of effective MCMC iterations to generate the joint quantile predictions.

---

distributions, we can draw samples from the posterior predictive distribution

$$p(\hat{Y}|Y) = \int p(\hat{Y}|\theta)p(\theta|Y)d\theta,$$

where  $\hat{Y}$  represents the set of values to forecast. Here, the posterior predictive distribution is not conditioned on parameter estimates or the inclusion/exclusion  
270 of predictors, all of which have been integrated out. Algorithm 2 conducts joint quantile prediction, where forecasts are generated by the Bayesian model averaging approach which provides a coherent mechanism to handle model uncertainty, by averaging the predicted values from all the models generated in the MCMC model training. Through Bayesian model averaging, we commit neither to any  
275 particular set of predictors which helps avoid an arbitrary selection, nor to point estimates of their coefficients which prevents overfitting.

## 5. Model Performance with Simulated Data

In this section, we demonstrate the model performance with simulated data generated by a three-dimensional target time series given in Section 5.1, in

280 terms of selecting the correct variables and accuracy in parameter estimation in  
 Section 5.2, and forecast performance of the model with different quantiles and  
 different time series correlations in Section 5.3.

### 5.1. Generated Data

The simulated data was generated by the following three-dimensional model

$$\tilde{y}_t = \tilde{\mu}_t + B^T \tilde{x}_t + \tilde{\epsilon}_t, \quad \tilde{\epsilon}_t \stackrel{iid}{\sim} \mathcal{AL}_3(\phi_\epsilon, \Sigma_\epsilon), \quad (35)$$

285 where each time series has its own trend component and regression component,  
 while quantiles and correlations are incorporated in the error term. That is,  
 with different quantiles and/or different correlations, we have different time  
 series datasets. Visualization of a part of a 3-dimensional time series dataset of  
 500 observations, generated by Model (35) with quantile  $\tau = (0.9, 0.9, 0.9)$  and  
 pairwise correlation  $\rho = 0.7$ , is given in Figure 1.

By the classical univariate case results in Yu and Moyeed (2001) and our  
 multivariate case illustrations in Section 2.2, the following deterministic trend  
 component guarantees that the regression coefficients  $B = B(\tau)$  are the exact  
 coefficients for quantile  $\tau$ :

$$\tilde{\mu}_{t+1} = \begin{bmatrix} \mu_{1,t+1} \\ \mu_{2,t+1} \\ \mu_{3,t+1} \end{bmatrix} = \begin{bmatrix} \mu_{1,t} \\ \mu_{2,t} \\ \mu_{3,t} \end{bmatrix} + \begin{bmatrix} \delta_{1,t} \\ \delta_{2,t} \\ \delta_{3,t} \end{bmatrix}, \quad \begin{bmatrix} \delta_{1,t} \\ \delta_{2,t} \\ \delta_{3,t} \end{bmatrix} = \begin{bmatrix} 0.04 + 0.6(\delta_{1,t-1} - 0.04) \\ 0.05 + 0.3(\delta_{2,t-1} - 0.05) \\ 0.02 + 0.1(\delta_{3,t-1} - 0.02) \end{bmatrix}.$$

The regression component was generated with 8 explanatory variables, at least  
 one of which has no effect on each target series with zero regression coefficient,  
 as follows:

$$B = \begin{bmatrix} 2 & 4 & -3.5 & -2 & 0 & 0 & -1.6 & 0 \\ 3 & 0 & 2.5 & -3 & 0 & -1.5 & 0 & 2 \\ -2.5 & 0 & -2 & -1 & 3 & 2 & 0 & 4 \end{bmatrix}^T,$$

$$\tilde{x}_t = \begin{bmatrix} x_{t1} & x_{t2} & x_{t3} & x_{t4} & x_{t5} & x_{t6} & x_{t7} & x_{t8} \end{bmatrix}^T,$$

$$x_{t1} \stackrel{iid}{\sim} \mathcal{N}(5, 5^2), \quad x_{t2} \stackrel{iid}{\sim} \text{Pois}(10), \quad x_{t3} \stackrel{iid}{\sim} \text{Pois}(5), \quad x_{t4} \stackrel{iid}{\sim} \mathcal{N}(-2, 5),$$

$$x_{t5} \stackrel{iid}{\sim} \mathcal{N}(-5, 5^2), \quad x_{t6} \stackrel{iid}{\sim} \text{Pois}(15), \quad x_{t7} \stackrel{iid}{\sim} \text{Pois}(20), \quad x_{t8} \stackrel{iid}{\sim} \mathcal{N}(0, 10^2).$$



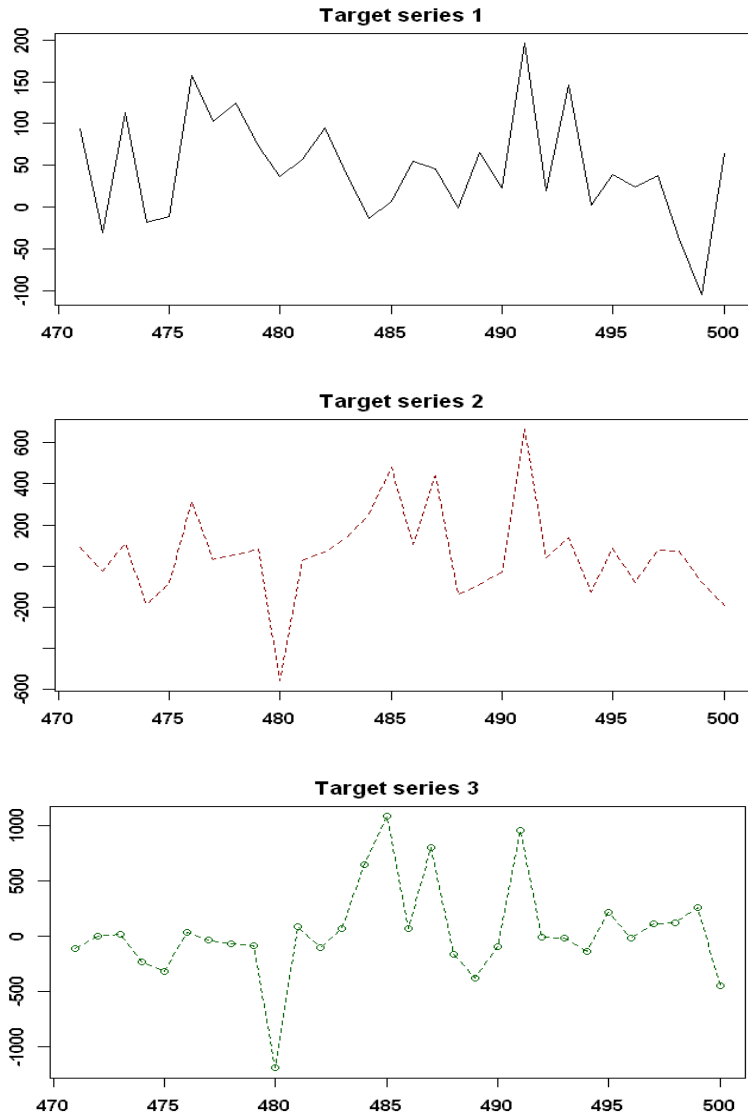


Figure 1: Target time series plot. Visualization of the last 30 observations of a 3-dimensional time series dataset of 500 observations, generated by Model (35) with quantile  $\tau = (0.9, 0.9, 0.9)$  and pairwise correlation  $\rho = 0.7$ .

The coefficients of the error term were generated by equation (14)

$$\phi_\epsilon = \Phi \tilde{\phi}_\tau, \quad \Sigma_\epsilon = \Phi \Sigma_\tau \Phi = \Phi (\Psi_\tau \Sigma_{\text{corr}} \Psi_\tau) \Phi,$$

where, for  $\tau = (\tau_1, \tau_2, \tau_3)$ ,

$$\Sigma_{\text{corr}} = \begin{bmatrix} 1 & \rho & \rho \\ \rho & 1 & \rho \\ \rho & \rho & 1 \end{bmatrix}, \quad \Phi = \begin{bmatrix} 0.7 & 0 & 0 \\ 0 & 0.6 & 0 \\ 0 & 0 & 0.9 \end{bmatrix},$$

$$\tilde{\phi}_\tau = \begin{bmatrix} \frac{2\tau_1-1}{\tau_1(1-\tau_1)} \\ \frac{2\tau_2-1}{\tau_2(1-\tau_2)} \\ \frac{2\tau_3-1}{\tau_3(1-\tau_3)} \end{bmatrix}, \quad \text{and} \quad \Psi_\tau = \begin{bmatrix} \sqrt{\frac{2}{\tau_1(1-\tau_1)}} & 0 & 0 \\ 0 & \sqrt{\frac{2}{\tau_2(1-\tau_2)}} & 0 \\ 0 & 0 & \sqrt{\frac{2}{\tau_3(1-\tau_3)}} \end{bmatrix}.$$

## 290 5.2. Model Training Performance

Machine learning models usually require large datasets to train, while in this section we are going to demonstrate the superior feature selection performances of the QFSTS model with small datasets, using only 400 MCMC iterations including 200 discarded as burn-in. The first three plots in Figure 2 provide the  
 295 feature selection results for a dataset of 500 observations, generated by Model (35) with quantile  $\tau = (0.9, 0.9, 0.9)$  and pairwise correlation 0.7. The threshold inclusion probability was set as 0.8, i.e.,  $\geq 80\%$  times a predictor was selected out of the  $(400 - 200)$  MCMC iterations. We can see that the selected features exactly match the model setup, where value 1 means a feature was selected all  
 300 the time out of the  $(400 - 200)$  MCMC iterations. The signs of selected variables also exactly match the model setup, and were marked with red for positive and blue for negative. The fourth plot of Figure 2 reveals that, for target series 3, only in a very small portion out of the  $(400 - 200)$  MCMC iterations, the model selected one more variable.

Figure 3 demonstrates the fast convergence and superior parameter estimation performance, with datasets generated by Model (35) with quantile  $\tau =$

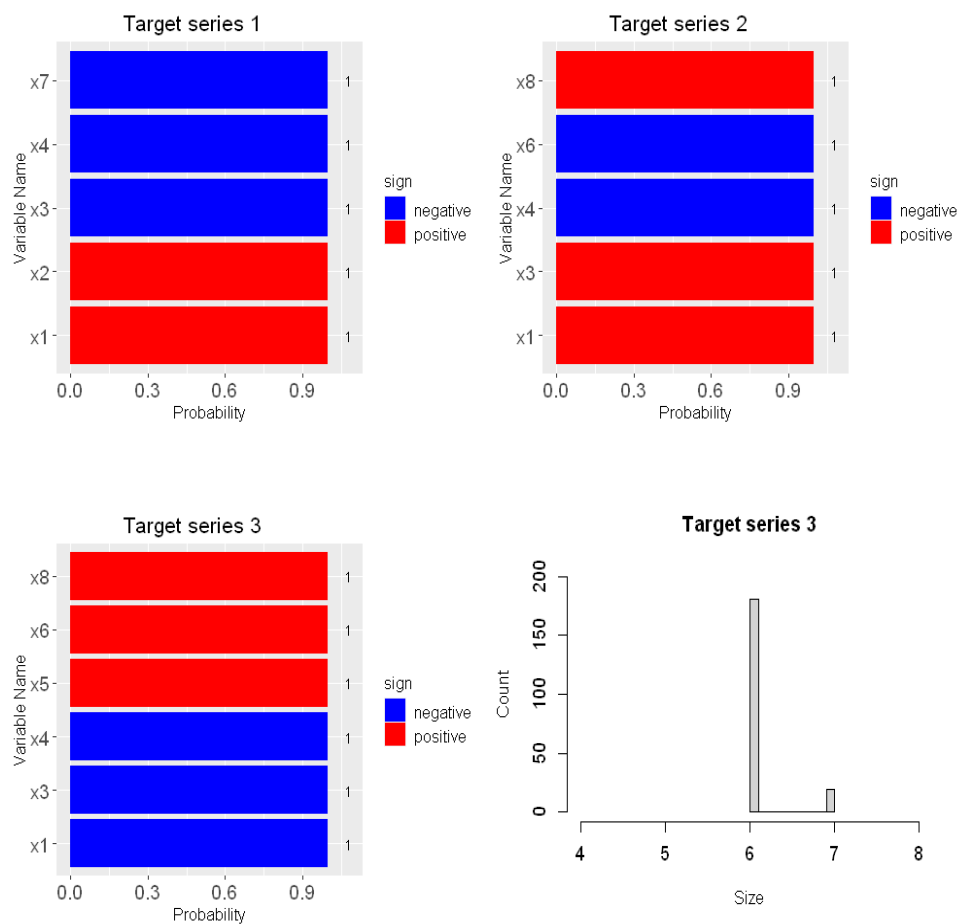


Figure 2: Feature selection results with simulated data. The 3-dimensional time series dataset of 500 observations was generated by Model (35) with quantile  $\tau = (0.9, 0.9, 0.9)$  and pairwise correlation 0.7. The threshold inclusion probability was set as 0.8. Model training used 400 MCMC iterations including 200 discarded as burn-in.

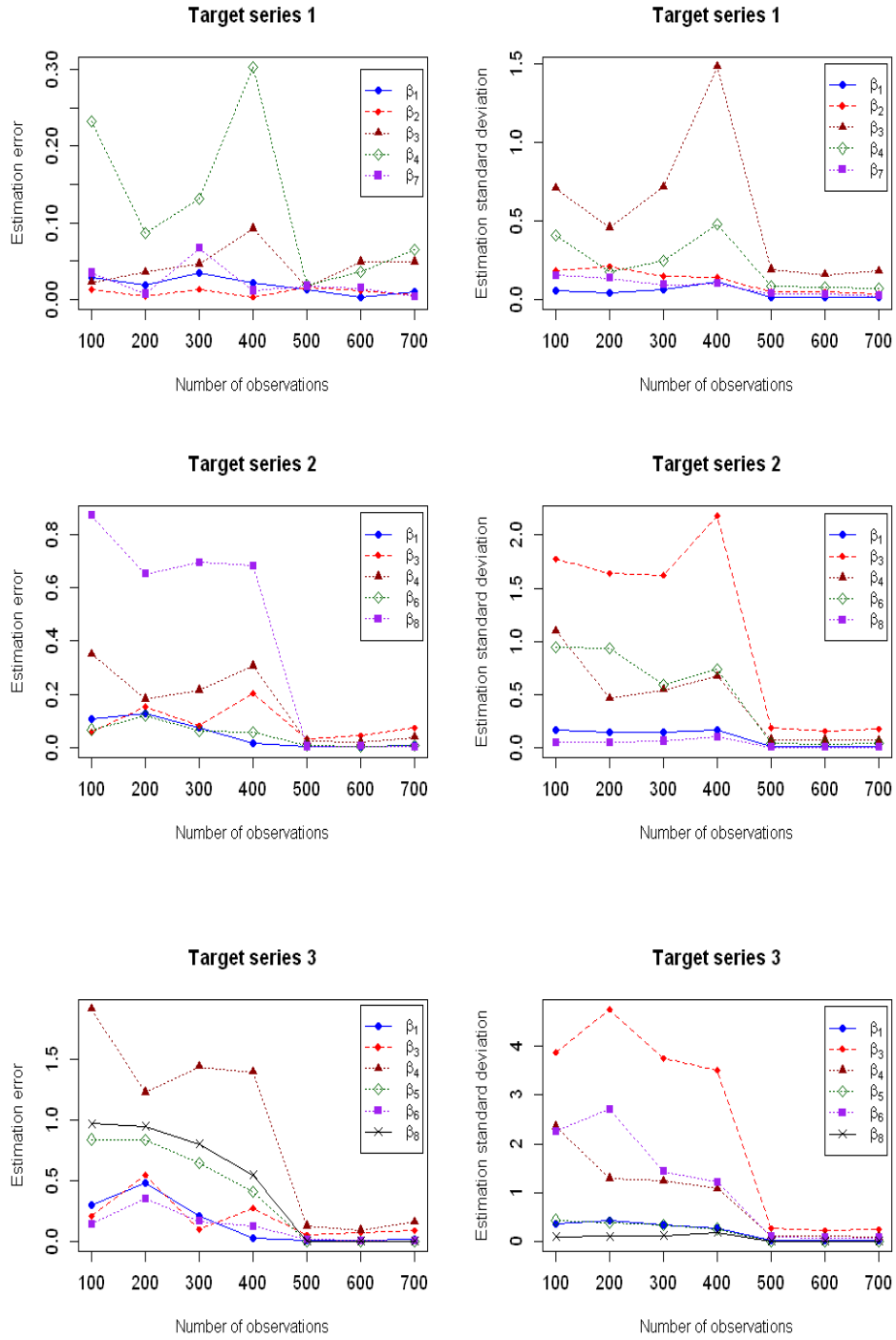


Figure 3: Estimation errors and standard deviations of regression coefficients. The 3-dimensional time series datasets were generated by Model (35) with quantile  $\tau = (0.9, 0.9, 0.9)$ , pairwise correlation  $\rho = 0.7$ , and 7 dataset sizes (100, 200, 300, 400, 500, 600, 700), using only 400 MCMC iterations including 200 discarded as burn-in.

(0.9, 0.9, 0.9), pairwise correlation  $\rho = 0.7$ , and 7 dataset sizes (100, 200, 300, 400, 500, 600, 700), using only 400 MCMC iterations including 200 discarded as burn-in. The left three plots provide the normalized estimation errors calculated as the

$$|(\text{estimated value} - \text{true value})/\text{true value}|,$$

305 and the right three plots provide the standard deviations of estimation. We can see that both the estimation errors and estimation standard deviations decrease fast as the sample size increases. Similar superior model training performances for different quantiles and correlations are implied in the forecast performance demonstrations in Section 5.3.

### 310 5.3. Forecast Performance

Quantile time series forecast is the prediction of the distribution of a future value of a time series. It is much more challenging than the time series mean or median forecast which is already difficult given the additional time information. For the quantile time series forecast, a prediction interval is generated as a range  
 315 of specified coverage probability under that forecast distribution. For example, the 95% prediction interval is defined by the 2.5% and 97.5% quantiles of the forecast distribution, and the 80% prediction interval is defined by the 10% and 90% quantiles of the forecast distribution. The most well-known quantile forecast algorithms that are publicly accessible approach, is the “auto.arima”  
 320 function for univariate time series analysis, in the “forecast” R package (Hyndman and Khandakar (2008)). “auto.arima” automatically fits the best ARIMAX Model, which is the most classical and popular time series model, according to either AIC, AICc or BIC value. Setting the “biasadj” option in the “auto.arima” function to “FALSE”, whose default value is “TRUE” for mean prediction, gives  
 325 the quantile prediction. There are only 4 quantile values possible: 2.5%, 10%, 90%, and 97.5%. Therefore, based on these 4 quantile values, we analyze the QFSTS model’s forecast performances.

Figure 4 reports the forecast performances for three-dimensional target time series datasets of 500 observations, generated by equation (35) with fixed pair-

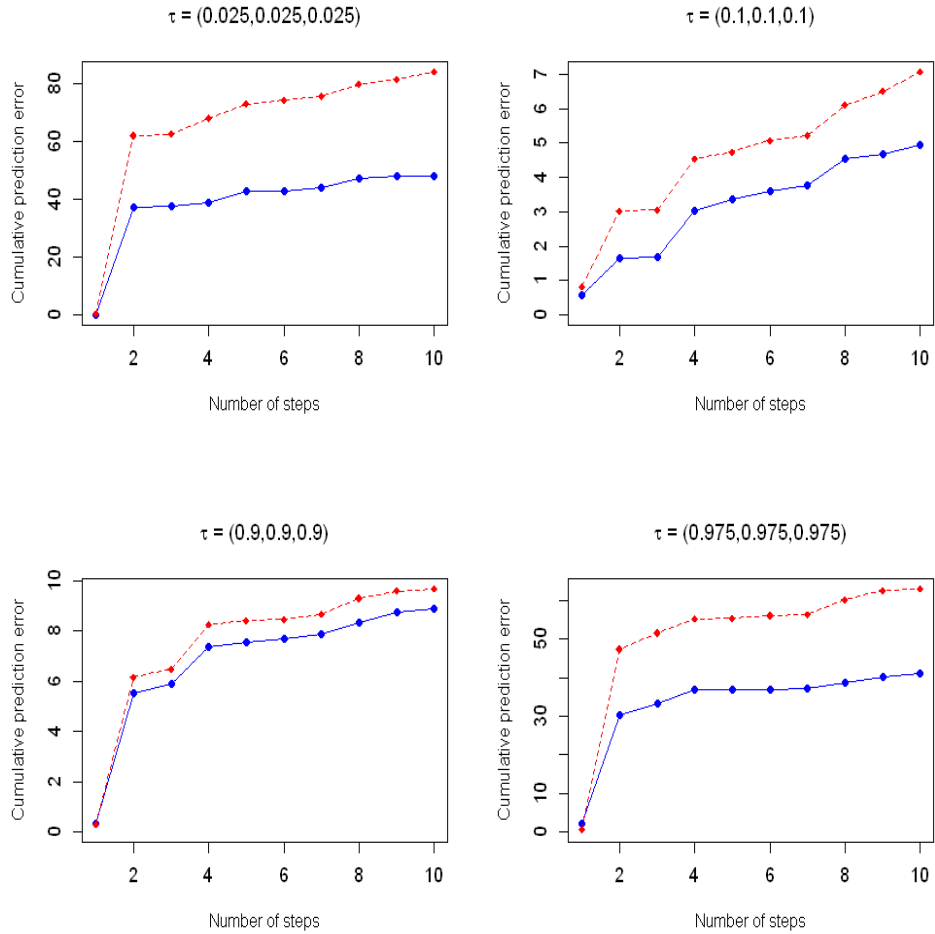


Figure 4: Cumulative absolute one-step-ahead prediction errors with simulated data for different quantiles. The red colored line is the performance of the ARIMAX model generated by “auto.arima” function, and the blue colored line is the performance of the QFSTS model. Three-dimensional time series datasets of 500 observations were generated by Model (35) with pairwise correlation  $\rho = 0.7$ . Model training used 400 MCMC iterations including 200 discarded as burn-in. Prediction error is measured by the quantile loss function given in equation (10).

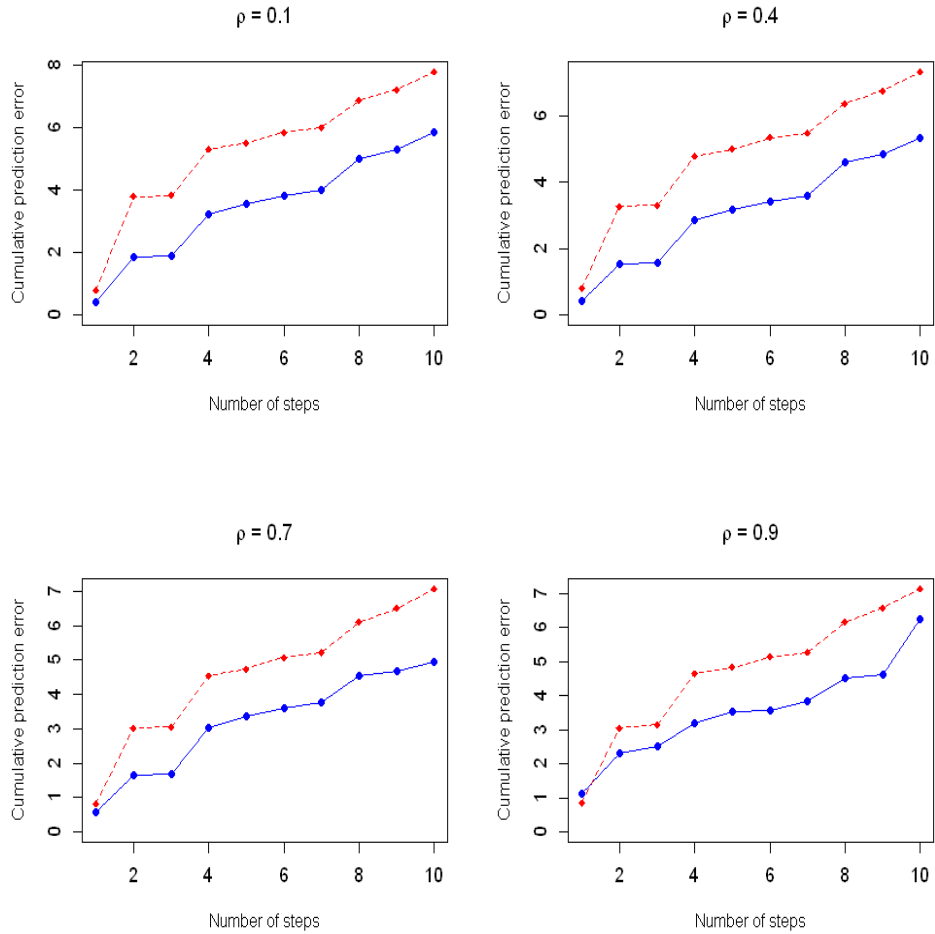


Figure 5: Cumulative absolute one-step-ahead prediction errors with simulated data for different pairwise correlations. The red colored line is the performance of the ARIMAX model generated by “auto.arima” function, and the blue colored line is the performance of the QFSTS model. Three-dimensional time series datasets of 500 observations were generated by Model (35) with fixed quantile  $\tau = (0.1, 0.1, 0.1)$ . Model training used 400 MCMC iterations including 200 discarded as burn-in. Prediction error is measured by the quantile loss function given in equation (10).

330 wise correlation  $\rho = 0.7$  but different quantiles:  $\tau = (0.025, 0.025, 0.025)$ ,  
 $\tau = (0.1, 0.1, 0.1)$ ,  $\tau = (0.9, 0.9, 0.9)$ , and  $\tau = (0.975, 0.975, 0.975)$ . The cu-  
mulative prediction error is calculated accumulatively according to the quantile  
loss function given in (10), where this standard approach can also be seen in  
Chen et al. (2013). We can see that the QFSTS model outperforms “auto.arima”  
335 consistently in the tens steps of one-step ahead forecast. Figure 5 reports the  
forecast performance for three-dimensional target time series datasets of 500  
observations, generated by Model (35) with fixed quantile  $\tau = (0.1, 0.1, 0.1)$   
but different pairwise correlations:  $\rho = 0.1$ ,  $\rho = 0.4$ ,  $\rho = 0.7$ , and  $\rho = 0.9$ .  
We can see that the QFSTS model outperforms “auto.arima” consistently in  
340 the ten steps of one-step ahead forecast with different multivariate time series  
correlations.

## 6. Model Performance with Empirical Data

For both Wall Street practitioners and financial researchers, to develop a  
strategy for trading and/or hedging purposes, most of the time one is going  
345 to work with time series data. Besides the mean prediction of multivariate  
financial time series, joint quantile prediction is extremely important. In finance  
terminology, Value at Risk (VaR) is a popular tool in the measurement and  
management of financial risk by providing a single number summarizing the  
total risk in a portfolio of financial assets (see Chap. 18 of Hull (2005)). It  
350 answers the question “How bad can things get?” by stating that “We are  
 $X$  percent certain that we will not lose more than  $V$  dollars in the next  $N$   
days”. Standard practice is to calculate VaR for a portfolio using a 1-day  
time horizon, a 95% confidence level, and 500+ days of historical data. In the  
following, we forecast the future values of price changes of a stock portfolio using  
355 the proposed QFSTS model and compare its performance with the benchmark  
ARIMAX model generated by the “auto.arima” function. The stock portfolio  
includes Bank of America (BOA), Capital One Financial Corporation (COF),  
JPMorgan Chase & Company (JPM), and Wells Fargo & Company (WFC).





Figure 6: Visualization of a part of the daily price change time series in 2017

Empirical data of 700 observations from 09/05/2014 to 06/16/2017 of daily  
 360 stock price changes, is free of charge and publicly available at Yahoo! Finance.  
 Visualization of a part of the historical sequence of price changes can be seen in  
 Figure 6.

Eight time series predictors are calculated for each company independently  
 as listed in Table 1, where the ChaVol indicator depicts volatility and measures  
 365 the difference between two moving averages of a volume-weighted accumulation  
 distribution line, the Vol indicator has the minimum estimation error and is

Variable	Abbr.
Chaikin volatility	ChaVol
Yang and Zhang Volatility historical estimator	Vol
Arms' Ease of Movement Value	EMV
Moving Average Convergence/Divergence	MACD
Money Flow Index	MFI
Aroon Indicator	AROON
Parabolic Stop-and-Reverse	SAR
Close Location Value	CLV

Table 1: Predictors

independent of drift and opening gaps, the EMV indicator is a momentum indicator to quantify the ease (or difficulty) of price movements, the MACD indicator is a trading indicator to reveal changes in the strength and duration of a trend in a stock's price, the MFI indicator is a ratio of positive and negative money flow over time and starts with the typical price for each period, the AROON indicator is used to identify trends in an underlying security and the likelihood that the trends will reverse, the SAR indicator is to find potential reversals in the market price direction of traded goods such as securities, and the CLV indicator is used to measure the close quote relative to the day's high and low.

There is no obvious trend in the target time series data, therefore we do not need the trend component in the QFSTS model. Figure 7 reports the feature selection results for these four banks, by setting the inclusion threshold probability as 0.7. We can see that the MACD indicator and the EMV indicator calculated with Bank of America's historical data are useful in explaining the movements of Bank of America's stock prices; the Vol indicator, the SAR indicator, the MFI indicator, the MACD indicator, and the EMV indicator calculated with Capital One Financial Corporation's historical data are useful in explaining the movements of Capital One Financial Corporation's stock prices; the

SAR indicator, the MFI indicator, the MACD indicator, and the EMV indicator calculated with JPMorgan Chase & Company’s historical data are useful in explaining the movements of JPMorgan Chase & Company’s stock prices; Wells Fargo & Company has the same important indicators as Capital One Financial Corporation, while those indicators generated with Wells Fargo & Company’s own historical data.

Figure 8 reports the forecast performance of different quantiles:  $\tau = (0.025, 0.025, 0.025)$  and  $\tau = (0.975, 0.975, 0.975)$  for VaR with 95% confidence level,  $\tau = (0.1, 0.1, 0.1)$  and  $\tau = (0.9, 0.9, 0.9)$  for VaR with 80% confidence level. As in the numerical analysis with simulated data, here the cumulative prediction error is calculated accumulatively according to the quantile loss function given in (10) (see, e.g., Chen et al. (2013)). We can see that the QFSTS model outperforms “auto.arima” consistently in the ten steps of one-step ahead forecast. We find that the errors of the QFSTS model accumulate much slower than “auto.arima”; “auto.arima” can have abrupt forecast failures at uncertain steps, such as the first step in low quantiles  $\tau = (0.025, 0.025, 0.025)$  and  $\tau = (0.1, 0.1, 0.1)$ , and the sixth step in high quantiles  $\tau = (0.9, 0.9, 0.9)$ , and  $\tau = (0.975, 0.975, 0.975)$ ; at the 95% prediction interval, i.e., at  $\tau = (0.025, 0.025, 0.025)$  and  $\tau = (0.975, 0.975, 0.975)$ , “auto.arima” has very high prediction errors.

## 7. Conclusion

In this paper, we have proposed the QFSTS model for the joint quantile time series analysis. The QFSTS model is a structural multivariate time series model, having a trend time series component, a regression component, and an error term. As a structural time series model, each component has its additional effects, and the QFSTS model can naturally be added on more components with additional effects. Accurate quantile feature selection is achieved by means of the “spike-and-slab” Bayesian prior setup, which uses the Bernoulli prior distribution for indicator variables. If no specific prior information on initial inclusion probabilities of particular variables is available, the Bernoulli

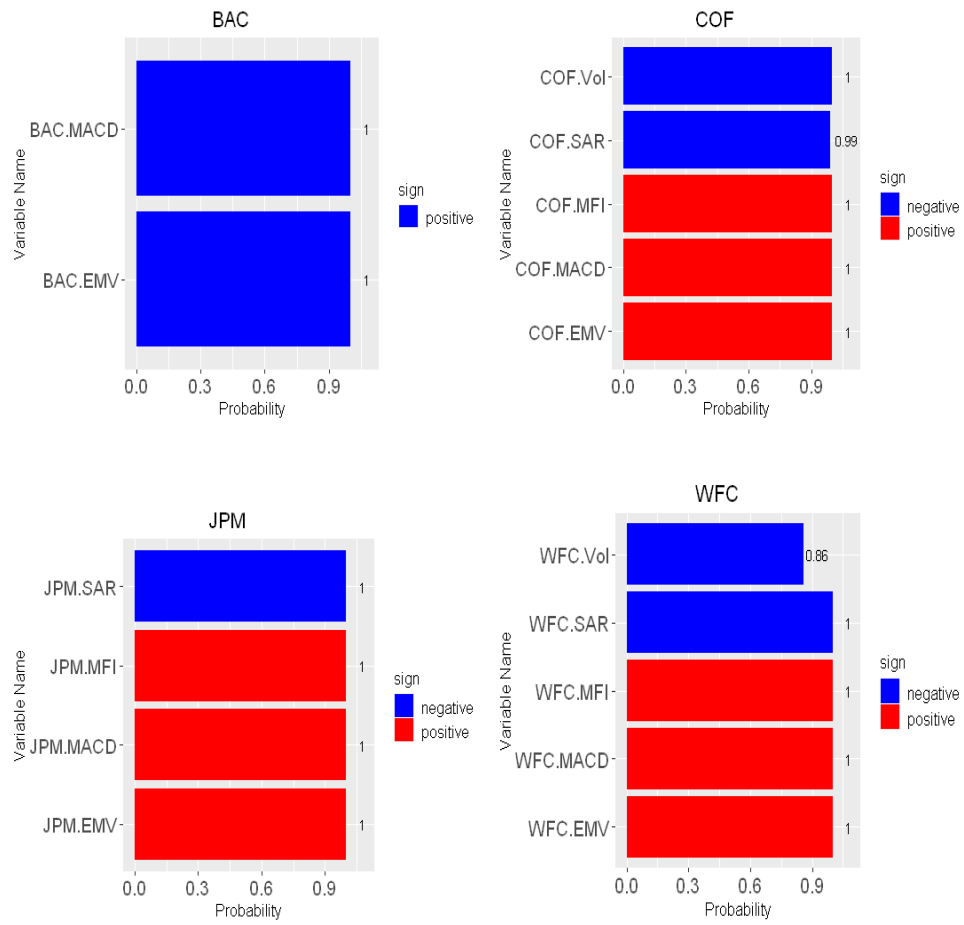


Figure 7: Feature selection results with empirical data for quantile  $\tau = (0.9, 0.9, 0.9)$ . The threshold inclusion probability was set as 0.7. Model training used 400 MCMC iterations including 200 discarded as burn-in.

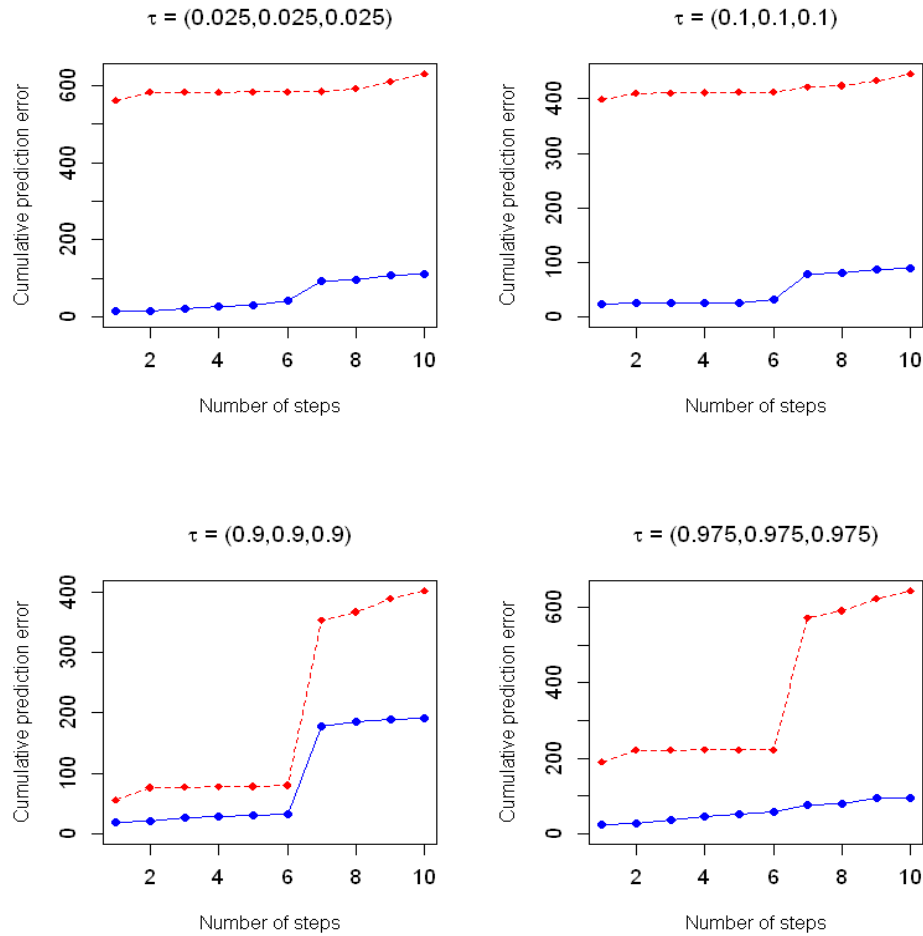


Figure 8: Cumulative absolute one-step-ahead prediction errors with empirical data for different sets of quantile values. The red colored line is the performance of the ARIMAX model generated by “auto.arima” function, and the blue colored line is the performance of the QFSTS model. Model training used 400 MCMC iterations including 200 discarded as burn-in. Prediction error is measured by the quantile loss function given in equation (10).

415 prior distribution is a common default choice. Variant “spike-and-slab” modeling can be used instead, such as “spike-and-slab” being normal distributions (George and McCulloch (1993)) or scale mixtures of normals (Ishwaran and Rao (2005)). The QFSTS model uses the standard Metropolis-Hastings algorithm in the MCMC model training while its speed and performance may be further  
420 improved with advanced Metropolis-Hastings algorithms (Banterle et al. (2019); Sherlock et al. (2017); Atchadé and Perron (2005); Atchadé et al. (2011)). As the first (univariate or multivariate) time series model with quantile feature selection, the QFSTS model sheds light on this new research area and outperforms the classical ARIMAX time series model consistently.

#### 425 **Acknowledgement**

The research of Ning Ning was partially supported by NSF grant DMS-1761603.

#### **References**

- Yves F Atchadé and François Perron. Improving on the independent Metropolis-  
430 Hastings algorithm. *Statistica Sinica*, pages 3–18, 2005.
- Yves F Atchadé, Gareth O Roberts, and Jeffrey S Rosenthal. Towards optimal scaling of Metropolis-coupled Markov chain Monte Carlo. *Statistics and Computing*, 21(4):555–568, 2011.
- Marta Banbura, Domenico Giannone, and Lucrezia Reichlin. Nowcasting. *The*  
435 *Oxford handbook of economic forecasting*, 2011.
- Marco Banterle, Clara Grazian, Anthony Lee, and Christian P Robert. Accelerating Metropolis–Hastings algorithms by delayed acceptance. *Foundations of Data Science*, 1(2):103, 2019.
- Kay H Brodersen, Fabian Gallusser, Jim Koehler, Nicolas Remy, and Steven L  
440 Scott. Inferring causal impact using Bayesian structural time-series models. *The Annals of Applied Statistics*, 9(1):247–274, 2015.

- Cathy WS Chen, David B Dunson, Craig Reed, and Keming Yu. Bayesian variable selection in quantile regression. *Statistics and its Interface*, 6(2): 261–274, 2013.
- 445 Victor Chernozhukov and Christian Hansen. An IV model of quantile treatment effects. *Econometrica*, 73(1):245–261, 2005.
- Victor Chernozhukov, Kaspar Wüthrich, and Zhu Yinchu. Exact and robust conformal inference methods for predictive machine learning with dependent data. In *Conference On Learning Theory*, pages 732–749. PMLR, 2018.
- 450 Nils Droste, Claudia Becker, Irene Ring, and Rui Santos. Decentralization effects in ecological fiscal transfers: a Bayesian structural time series analysis for Portugal. *Environmental and Resource Economics*, 71(4):1027–1051, 2018.
- James Durbin and Siem Jan Koopman. A simple and efficient simulation smoother for state space time series analysis. *Biometrika*, 89(3):603–616, 455 2002.
- Edward I George and Robert E McCulloch. Variable selection via Gibbs sampling. *Journal of the American Statistical Association*, 88(423):881–889, 1993.
- Edward I George and Robert E McCulloch. Approaches for Bayesian variable selection. *Statistica sinica*, pages 339–373, 1997.
- 460 Søren Hauberg, François Lauze, and Kim Steenstrup Pedersen. Unscented Kalman filtering on Riemannian manifolds. *Journal of mathematical imaging and vision*, 46(1):103–120, 2013.
- Jennifer A Hoeting, David Madigan, Adrian E Raftery, and Chris T Volinsky. Bayesian model averaging: a tutorial. *Statistical science*, pages 382–401, 1999.
- 465 Peter J Huber. *Robust statistics*, volume 523. John Wiley & Sons, 2004.
- John Hull. *Options, futures and other derivatives (6th edition)*. Upper Saddle River, NJ: Prentice Hall, 2005.

- Rob J. Hyndman and Yeasmin Khandakar. Automatic time series forecasting: The forecast package for R. *The Annals of Statistics*, 27(3), 2008.
- 470 Hemant Ishwaran and J Sunil Rao. Spike and slab variable selection: Frequentist and Bayesian strategies. *The Annals of Statistics*, 33(2):730–773, 2005.
- Akanksha Jalan, Roman Matkovskyy, and Andrew Urquhart. What if bitcoin futures had never been introduced? *Available at SSRN 3491272*, 2019.
- S Rao Jammalamadaka, Jinwen Qiu, and Ning Ning. Predicting a stock portfolio with the multivariate Bayesian structural time series model: Do news or  
475 emotions matter? *International Journal of Artificial Intelligence*, 17(2):81–104, 2019.
- Yu Jiang, Zhe Song, and Andrew Kusiak. Very short-term wind speed forecasting with Bayesian structural break model. *Renewable energy*, 50:637–647,  
480 2013.
- Bent Jorgensen. *Statistical properties of the generalized inverse Gaussian distribution*, volume 9. Springer Science & Business Media, 2012.
- Samuel Kotz, Tomasz Kozubowski, and Krzysztof Podgorski. *The Laplace distribution and generalizations: A revisit with applications to communications, economics, engineering, and finance*. Springer Science & Business Media,  
485 2012.
- Anastasis Kratsios and Cody Hyndman. Neu: A meta-algorithm for universal uap-invariant feature representation. *Journal of Machine Learning Research*, 22(92):1–51, 2021.
- 490 Christoph F Kurz, Martin Rehm, Rolf Holle, Christina Teuner, Michael Laxy, and Larissa Schwarzkopf. The effect of bariatric surgery on health care costs: A synthetic control approach using Bayesian structural time series. *Health economics*, 28(11):1293–1307, 2019.



- David Madigan and Adrian E Raftery. Model selection and accounting for  
495 model uncertainty in graphical models using Occam’s window. *Journal of the  
American Statistical Association*, 89(428):1535–1546, 1994.
- Laetitia Papaxanthos, Felipe Llinares-López, Dean Bodenham, and Karsten  
Borgwardt. Finding significant combinations of features in the presence of  
categorical covariates. In *Advances in neural information processing systems*,  
500 pages 2279–2287, 2016.
- Jinwen Qiu, S Rao Jammalamadaka, and Ning Ning. Multivariate Bayesian  
structural time series model. *The Journal of Machine Learning Research*, 19  
(1):2744–2776, 2018.
- Jinwen Qiu, Wenjian Liu, and Ning Ning. Evolution of regional innovation  
505 with spatial knowledge spillovers: Convergence or divergence? *Networks and  
Spatial Economics*, pages 1–30, 2019.
- Jinwen Qiu, S Rao Jammalamadaka, and Ning Ning. Multivariate time series  
analysis from a Bayesian machine learning perspective. *Annals of Mathemat-  
ics and Artificial Intelligence*, 88(10):1061–1082, 2020.
- 510 Christian P Robert and George Casella. *Introducing Monte Carlo Methods with  
R*, volume 18. Springer, 2010.
- Steven L Scott and Hal R Varian. Predicting the present with Bayesian struc-  
tural time series. *International Journal of Mathematical Modelling and Nu-  
merical Optimisation*, 5(1-2):4–23, 2014.
- 515 Steven L Scott and Hal R Varian. Bayesian variable selection for nowcasting  
economic time series. In *Economic analysis of the digital economy*, pages  
119–135. University of Chicago Press, 2015.
- Chris Sherlock, Alexandre H Thiery, and Anthony Lee. Pseudo-marginal  
Metropolis–Hastings sampling using averages of unbiased estimators.  
520 *Biometrika*, 104(3):727–734, 2017.

- Amir Talaei-Khoei, Madjid Tavana, and James M Wilson. A predictive analytics framework for identifying patients at risk of developing multiple medical complications caused by chronic diseases. *Artificial Intelligence in Medicine*, 101:101750, 2019.
- 525 Hal R Varian. Big data: New tricks for econometrics. *The Journal of Economic Perspectives*, 28(2):3–27, 2014.
- Kasper Welbers and Michaël Opgenhaffen. Social media gatekeeping: An analysis of the gatekeeping influence of newspapers’ public Facebook pages. *new media & society*, 20(12):4728–4747, 2018.
- 530 Yiqing Xu. Generalized synthetic control method: Causal inference with interactive fixed effects models. *Political Analysis*, 25(1):57–76, 2017.
- Keming Yu and Rana A Moyeed. Bayesian quantile regression. *Statistics & Probability Letters*, 54(4):437–447, 2001.